The Permian Cornubian granite batholith, SW England; Part 1: Field, structural, and petrological constraints

Michael P. Searle[1,2,3], Robin K. Shail[1], Jonathan M. Pownall[3,4], Christopher Jurkowski[3], Anthony B. Watts[3], and Laurence J. Robb[3]

[1]*Camborne School of Mines, Department of Earth and Environmental Science, University of Exeter (Penryn campus), Penryn, Cornwall TR10 9FE, UK*

[2]*Oxford University Museum of Natural History, Parks Road, Oxford OX1 3PW, UK*

[3]*Department of Earth Sciences, University of Oxford, South Parks Road, Oxford OX1 3AN, UK*

[4]*Department of Geosciences and Geography, University of Helsinki, Gustaf Hällströmin katu, 00014 Helsinki, Finland*

ABSTRACT

The Permian Cornubian granite batholith (295–275 Ma) in SW England includes seven major plutons and numerous smaller stocks extending for ~250 km from the Isles of Scilly in the WSW to Dartmoor in the ENE. The granites are peraluminous and classified as crustal melt S-type, predominantly two-mica granites, and biotite or tourmaline monzo and syenogranites, with subordinate minor topaz granite and lithium mica granite. The granites and their host rocks are pervasively mineralized with tin (cassiterite), tungsten (wolframite, ferberite), copper (chalcopyrite, chalcocite, bornite), arsenic (arsenopyrite), and zinc (sphalerite) mineralized lodes. Quartz-muscovite selvedges (greisen-bordered) also contain enrichment of lithophile elements such as boron (tourmaline), fluorine (fluorite), and lithium (lithium-micas such as lepidolite and zinnwaldite). They are derived from both muscovite and biotite dehydration melting of pelitic-psammitic rocks and intruded from a common source along the length of the batholith. Pressure estimates from andalusite and cordierite-bearing hornfels in the contact metamorphic aureole (150 ± 100 MPa) show that the granites intruded to 3 km depth. Cupolas around the Land's End and Tregonning granites show aplite-pegmatite dikes and tourmaline + quartz + muscovite veins (greisen) that are frequently mineralized. Synchronous intrusions of lamprophyre dikes suggest an additional heat source for crustal melting may have been from underplating of alkaline magmas. The lack of significant erosion means that the source region is not exposed. In an accompanying paper (Part 2; Watts et al., 2024), gravity modeling reveals possible solutions for the shape and depth of the granite and the structure of the lower crust. We present a new model for the Land's End, Tregonning, and Carnmenellis granites showing a mid-crustal source composed of amphibolite facies migmatites bounded by prominent seismic reflectors, with upward expanding dikes feeding inter-connected granite laccoliths that show inflated cupolas with shallow contact metamorphism. The Cornubian granites intruded >90 m.y. after obduction of the Lizard ophiolite complex, and after Upper Devonian–Carboniferous Variscan compressional, and later extensional, deformation of the surrounding Devonian country rocks. Comparisons are made between the Cornubian batholith and the Patagonian batholith in Chile, the Himalayan leucogranites, and the Baltoro granite batholith along the Karakoram range in northern Pakistan.

1. INTRODUCTION

During orogenesis, melting of the lower regions of continental crust and granitic emplacement into the middle and upper crust is the major process by which the crust has differentiated into a mafic, dry, residual lower crust and a more felsic, hydrated upper crust (Read, 1948; Brown and Rushmer, 2006; Brown, 2007, 2013). Two granite end-members are: (1) lower (or lower/ mid) crustal, mantle-derived, metaluminous, I-type granites, typically formed inboard of subduction zones such as the Andes by high-temperature melting to form hornblende-rich (+ titanite, magnetite) tonalites-granodiorites, as well as more fractionated compositions that can reach the surface to form porphyry systems (e.g., Clemens et al., 2011; Bonin et al., 2020; Jacob et al., 2021), which are also termed the magnetite-series granites (Ishihara, 1977), and (2) mid-crustal sourced, peraluminous S-type granites derived from melting of pelitic-psammitic meta-sedimentary and migmatite rocks, such as those formed along the Himalaya, by lower temperature melting in a migmatitic source region. These granites are the end product of regional Barrovian-type metamorphism, contain magmatic minerals such as garnet (Grt), muscovite (Ms), biotite (Bt), tourmaline, cordierite (Crd), and may contain andalusite (Als) and sillimanite in the melt (Chappell and White, 1974; White and Chappell, 1977; Clemens, 2003, 2012), and are also termed the ilmenite-series granites (Ishihara, 1977). Magnetite series granites may be associated with porphyry copper-molybdenum mineralization, whereas ilmenite series granites frequently host tin-tungsten deposits. A third category, the A-type (alkaline) granites are anorogenic and are thought to result from localized high-temperature melting of a lower crust granulite source (Collins et al., 1982; Whalen et al., 1987).

Granite emplacement processes involving the transfer of melts from the lower or middle crust to the upper crust remain controversial. Early models involved the vertical ascent of magmas as diapirs (e.g., Bott et al., 1958; Willis-Richards and Jackson, 1989; Weinberg and Podladkicov, 1994; Burov et al., 2003). Later models involved processes such as compaction-driven melting to form a network of veins and channels (Brown and Solar, 1998; Weinberg and Searle, 1998, 2013; Weinberg and Mark, 2008; Searle et al., 2009; Sawyer et al., 2011), diking (Clemens and Mawer, 1992; Petford et al., 1993), emplacement by stoping and assimilation (Glazner and Bartley, 2006), emplacement into extensional or trans-tensional shear zones (Hutton and Reavy, 1992), emplacement into transpressional shear zones (Searle et al., 2016), and lateral emplacement as laccoliths or horizontal tabular intrusions (Cruden, 1998; Taylor, 2007). Mountain belts usually show limited depth exposures depending on their age and erosion levels. Only a few mountain belts, such as the Himalaya (e.g., Searle et al., 1997, 2009; Searle, 2016; Weinberg and Searle, 1999) and Karakoram (Searle et al., 2010; Weinberg and Searle, 1998; Weinberg and Mark, 2008), show a complete structural profile from source to high-level granite, due to crustal-scale tilting and deep erosion. These S-type crustal melt granites are derived from regional metamorphic-migmatite terrains with in situ melting of a dominantly metapelitic source at sillimanite grade, followed by intrusion via a dike-sill network to higher level intrusions.

Two parallel granitic batholiths are present in SW England (Fig. 1) and the adjacent offshore continental shelf, first the main Cornubian batholith of Permian age, cropping out from the Isles of Scilly, through mainland Cornwall and west Devon, and second, the Haig Fras batholith, also of Permian age, that crops out as submerged reefs to the NW of the Isles of Scilly as evidenced from a large gravity anomaly (Fig. 1). Granites from the Haig Fras reefs have been dredged, but not directly sampled (Jones et al., 1988). Farther east, offshore from North Devon, the Lundy granite has a mineralogy and peraluminous geochemistry similar to the Permian Cornubian batholith granites,

but has a Paleocene U-Pb zircon age of 59.8–58.4 ± 0.4 Ma and represents Atlantic opening rift-related and plume-related magmatism (Charles et al., 2018).

In this paper we first review the wealth of previous data on the Cornubian granite batholith, notably the field relationships, structure, petrology, U-Pb zircon ages, mineralization, and contact metamorphic aureole around the granites, as well as synchronous lamprophyre dikes. We also review the models proposed for the deep structure, from early models of diapiric plutons (De La Beche, 1839; Bott et al., 1958) to later models of dike-fed laccoliths (Taylor, 2007). We then review the composition and structure of the seven major plutons along the Cornubian batholith. Only the uppermost structural levels of the plutons are exposed, so it is necessary to infer the structure of the batholith and middle-lower crust from gravity and seismic data.

Seismic refraction and reflection surveys by Brooks et al. (1984) and Jones (1991) revealed two prominent reflectors R1 and R2 at depths of 8 km and ∼15 km. A third reflector R3, at a depth of ∼28 km, was interpreted as the Moho. Bott et al. (1958) and Willis-Richards and Jackson (1989) proposed a model of diapiric plutonism rising from a regionally connected mid-crustal granite batholith, based on structures observed from gravity modeling. They modeled outward-dipping flanks of the plutons to depths of 10–12 km. The base of the granites is unknown but is likely to be a zone of high-grade meta-sedimentary gneisses and migmatites. In Part 2 (Watts et al., 2024), we use gravity data to constrain the shape of the batholith at depth. We combine these data to present a new model for the shape of the Cornubian granite batholith in the Land's End, Tregonning, and Carnmenellis region, as well as to discuss various emplacement mechanisms, comparing these features with similar large granite bodies in Patagonia, the Himalaya, and Karakoram.

2. CORNUBIAN GRANITE BATHOLITH

The Cornubian batholith extends from the Isles of Scilly in the west to Dartmoor in the east (250 km long × 20–40 km wide) and is a single continuous batholith (Bott et al., 1958; Willis-Richards and Jackson, 1989). Seven major plutons are exposed in Cornwall and west Devon represented by the Isles of Scilly, Land's End, Tregonning-Godolphin, Carnmenellis, St Austell, Bodmin Moor, and Dartmoor granites, as well as several smaller stocks and plugs such as St Michael's Mount (Penzance), Cligga Head, St Agnes, Castle an Dinas, Kit Hill, and Hemerdon (Fig. 1). U-Pb zircon and monazite dating shows that the Cornubian granites are Early Permian ranging between ca. 295 Ma and 275 Ma (Fig. 2; Chen et al., 1993; Chesley et al., 1993; Smith et al., 2019). The total volume of the batholith has been estimated as 68,000 km^3 (WillisRichards and Jackson, 1989), although neither the shape of individual plutons at depth nor the nature of the lower contact of the granites is well constrained. More accurate geophysical constraints are given in Part 2 (Watts et al., 2024).

The Cornish granites are remarkably heterogeneous and display large mineralogical, textural, and chemical variations within a single pluton. They are generally classified as peraluminous (molecular proportion Al_2O_3 > (Na_2O + K_2O + CaO)) crustal, S-type monzogranites and syenogranites. Coarse-grained megacrystic two-mica, biotite, and tourmaline granites form the main types, with localized magmatic-hydrothermal intrusions of topaz granites and lithium mica granites. The granites are rich in tin (Sn) as cassiterite, tungsten (W) as wolframite and ferberite, boron (B) in tourmaline, fluorine (F) in fluorite, and lithium (Li) in lithium-micas such as lepidolite and zinnwaldite (Exley and Stone, 1982; Stone and Exley, 1985; Willis-Richards and Jackson, 1989; Floyd et

al., 1993; Chappell and Hine, 2006; Simons et al., 2016, 2017; Smith et al., 2019). Granites were formed by partial melting of continental crust, and preserve a complete spectrum of processes from magmatic to hydrothermal. Sn and W were sourced from magmatic-hydrothermal fluids, and concentrated into highly altered "greisen" veins and quartz-tourmaline and quartz-chlorite-sulfide lodes (Bromley and Holl, 1986; Willis-Richards and Jackson, 1989; Jackson et al., 1989; Sams and Thomas-Betts, 1988; Chesley et al., 1993; Williamson et al., 2010). Extensive alteration of feldspars also resulted in widespread argillic alteration, forming the kaolin china clay (kaolinite) deposits mined around SW Dartmoor and St Austell (Manning et al., 1996).

Granite emplacement post-dates regional folds, faults and cleavage, formed during Late Devonian and Carboniferous Variscan convergence, and subsequent late Carboniferous–Permian post-orogenic extension (Shail and Wilkinson, 1994; Shail et al., 2003; Hughes et al., 2009; Alexander et al., 2019). The granites are peraluminous and derived from partial melting of a feldspathic pelitepsammite sedimentary source (Chappell and Hine, 2006; Müller et al., 2006; Simons et al., 2016, 2017; Clemens, 2012). The oldest granites (295–288 Ma) are the two-mica granites (e.g., Isles of Scilly, Carnmenellis, Bodmin) and muscovite granites (Hemerdon), whereas the younger granites (284–275 Ma) are represented by the composite biotite and tourmaline granites of Dartmoor, St Austell, and Land's End (Smith et al., 2019). Simons et al. (2016) proposed a two-stage model where the older granites formed by muscovite-dehydration melting at pressure-temperature (P-T) conditions of 730–800 °C and >500 MPa. Later melting at higher temperature and lower pressure resulted in melting of more refractory minerals and generation of the biotite granites, which fractionated to form the tourmaline granites.

Since only the upper parts of the granites are exposed, the nature of the source region and the source rocks remains unknown. The major questions we attempt to answer here and in Part 2 (Watts et al., 2024) are: (1) What is the shape of the batholith (diapiric plutons that rose from a conjoined granite base, or dike-fed upper crustal laccoliths)? (2) What is the nature of the lower contact of the granite (structural, or gradational from a migmatite source)? (3) What is the nature of the granite margins (narrowing downward, or narrowing upward)? (4) What are the emplacement mechanisms (vertical diapirism, fracturedike propagation, stoping, lateral magma transport along sills or laccoliths)?

Variscan and Post-Variscan Tectonics and Host-Rock Relations

SW England preserves a record of the development of the narrow Devonian Rhenohercynian Ocean basin along the northern margin of, or as a successor basin to, the Rheic Ocean (Franke, 2024). Pre-Devonian basement is poorly constrained; while an Avalonian provenance is commonly assumed, other peri-Gondwana terranes might have been accreted at the southern margin of Avalonia prior to Rhenohercynian rifting (e.g., Woodcock et al., 2007; Nance et al., 2015; Dijkstra and Hatch, 2018).

Variscan convergence in SW England occurred from the Late Devonian to the late Carboniferous. In the south, peak-convergencerelated deformation (D1) occurred during the Late Devonian to earliest Carboniferous (Famennian to Tournaisian, 370–360 Ma). It was related to accretionary processes accompanying the southward subduction of oceanic lithosphere and formation of the seismically defined S-dipping Rhenohercynian suture to which SW England

represents the lower plate (e.g., Le Gall, 1990; Shail and Leveridge, 2009; Alexander et al., 2019). Farther north, on the SW England proximal passive margin, Variscan primary deformation (D1) brought about thick-skinned inversion of Devonian and Carboniferous successions during the Visean to Serpukhovian (ca. 345–325 Ma; Leveridge and Hartley, 2006). Late Carboniferous Variscan (D2) convergence resulted in NNW-directed thrusting across the region during the Moscovian to Kazimovian (ca. 315–305 Ma; Leveridge and Hartley, 2006). A change in plate-boundary stresses occurred across NW Europe during the latest Carboniferous, as Variscan convergence was replaced by a dextral transtensional post-Variscan regime, manifest by displacements on major NW-SE– striking faults (e.g., Ziegler and Dèzes, 2006). In SW England, dextral movements on NW-SE– striking faults were accompanied by the coeval extensional reactivation of ENE-WSW– to E-W–striking Variscan thrust faults in the basement and the Rhenohercynian suture (Shail and Leveridge, 2009; Alexander et al., 2019).

Field relations indicate that the felsic igneous rocks of the Cornubian Batholith always post-date Variscan convergence-related D1 and D2 structures in the Devonian and Carboniferous host rocks. Post-Variscan ductile D3 structures in the host rocks, comprising SSEor S-verging folds and associated cleavages, and/ or fault systems displaying a top-to-the-south sense-of-shear, are truncated by pluton margins, cut by undeformed granite and aplite sheets, and included within host rock enclaves (Stone, 1971). These relations are consistent with ductile D3 deformation, controlled by the post-Variscan NNW-SSE extensional reactivation of thrust faults, occurring prior to the emplacement of the younger granites (Alexander and Shail, 1995, 1996; Hughes et al., 2009). The host rocks, older and younger granites are collectively cut by high-angle faults and joints, developed during ongoing early post-Variscan NNW-SSE extension, that host magmatic-hydrothermal mineralization (Shail and Wilkinson, 1994; Alexander and Shail, 1995, 1996; Shail and Leveridge, 2009; Hughes et al., 2009). All the Cornubian granites were, therefore, generated and emplaced in a post-orogenic extensional tectonic regime (Shail et al., 2003). D3 and earlier structures were tilted away from the plutons during emplacement, particularly along their northern margins, to define broad open antiforms (Rattey and Sanderson, 1984; Hughes et al., 2009). Bedding, metabasic rocks, and the trace of S1 cleavage locally define marginal synclines around the northern parts of Carnmenellis, St Austell, Bodmin Moor, and Dartmoor granites interpreted to reflect emplacement-related roof uplift (Taylor, 2007). NW-dipping faults along the northern margin of the batholith have also been invoked as accommodating pluton growth (Alexander and Shail, 1995).

Granite Composition

The peraluminous Cornubian granites are rich in alkali major elements and Rb, Li, B, F, Nb, Sn, are associated with tin and tungsten mineralization, and are thus typical S-type granites, derived from melting of a sedimentary source (Willis-Richards and Jackson, 1989; Floyd et al., 1993; Chappell and Hine, 2006). They are enriched in high heat-producing elements (U, Th, K) and have elevated $^{87}Sr/^{86}Sr$ ratios (Darbyshire and Shepherd, 1985, 1994). However, the Dartmoor granite uniquely contains rare enclaves with hornblende and titanite, a restitic assemblage that is usually associated with I-type granites (Stimac et al., 1995). This could be used to argue for a minor mantle-derived mafic component, rather than a pure crustal origin (Darbyshire and Shepherd, 1994; Stimac

et al., 1995). Alternatively, it could be argued that the granites are more representative of post-orogenic alkalic A-type magmatism associated with simultaneous intrusion of lamprophyre dikes.

The Permian granites of SW England are clearly not equivalent to I-type, Andean subduction-related granites (Pitcher, 1979), as they have no hornblendebearing diorite-granodiorite magma phases and are both potassic and peraluminous, rich in alumino-silicates and K-feldspar (Kfs). They are petrographically similar to S-type Himalayan leucogranites containing K-feldspar, quartz (Qtz), biotite, muscovite, garnet, tourmaline, and cordierite as magmatic phases (Searle et al., 2009), but they are structurally unlike the Himalayan leucogranites, which have a vast migmatite base and intrude as sills and dikes into sillimanite grade country rocks.

The two relevant melt reactions that describe the formation of Cornubian-type granites are the fluid-absent melt-producing muscovite dehydration reaction leading to leucogranite formation

$$Ms \pm Bt + plagioclase\ (Pl) + Qtz = Als \pm Grt + Kfs + melt \quad (1)$$

and the higher temperature biotite dehydration reaction leading to monzogranite formation

$$Bt + Pl + Als + Qtz = Grt \pm Crd + Kfs + melt \quad (2)$$

Restitic orthopyroxene and hornblende are never seen in Cornubian granite melts, so it appears that crustal melting occurred in the upper amphibolite facies middle crust, rather than the granulite facies restitic lower crust.

The Cornubian granites have been classified into five main types (Simons et al., 2016, 2017):

G1—Two-mica granites with microperthite phenocrysts, formed by muscovite (and minor biotite) dehydration melting of a greywacke source at 730–800 °C and >5 kbar. These granites form the main constituents of the Isles of Scilly, Carnmenellis, and Bodmin Moor granites (Charoy, 1986; Simons et al., 2016).

G2—Muscovite granites, with occasional cordierite, are typically peraluminous granites, and formed from fractionation of G1 granites. Fractionation enriched these granites in Li, Ta, and rare earth elements (REEs). They are typically represented by stocks, such as the Hemerdon and Cligga Head granites, where they host Sn and W mineralization in the greisen-bordered quartz + muscovite vein systems such as at Cligga Head stock.

G3—Biotite-cordierite granites with large K-feldspar phenocrysts and increased tourmaline content form the major plutons of Land's End, Dartmoor, and parts of the St Austell granite. They were formed by biotite dehydration melting at slightly higher temperatures and lower pressures, ~760–850 °C and <4 kbar, respectively (Simons et al., 2016), and are enriched in boron that is manifested by a higher tourmaline content. Older biotite + K-feldspar megacrystic granites are enclosed by younger tourmaline granites and lithium mica-albite granites (Müller et al., 2006).

G4—Tourmaline granites with coarse-grained quartz and K-feldspar and lithium-enriched micas, derived by fractionation from biotite granites, represent a significant component of the Land's End and St Austell granites. Tourmaline and biotite are not mutually exclusive. Tourmaline schorl + quartz granites are present at Roche rock along the northern margin of the St Austell pluton (Williamson et al., 2000) and at Luxulyan quarry.

G5—Topaz granites contain fine-grained quartz, microperthite, tourmaline, and zinnwaldite/lepidolite lithium-micas, have high topaz contents, and are restricted to the Tregonning granite and the Hensbarrow and Nanpean stocks in the St Austell granite (Stone, 1992; Manning et al., 1996; Simons et al., 2016; Breiter et al., 2018). They are associated with rare metal banded pegmatite-aplite sills at Megiliggar Rocks. Mineralogical diversity has been explained by the exsolution of separate Na-LiFl-rich and K-B-rich fluid phases from the primary melt (Breiter et al., 2018). Manning et al. (1996) and Simons et al. (2016) suggested that the topaz granites are compositionally distinct, were not related to other granites by fractional crystallization, but were derived by granulite facies melting of a biotite-rich protolith in the lower crust. The presence of extensive lithium micas (lepidolite, zinnwaldite) and the association with fluids rich in F, Li, P, and high field strength elements, however, suggest that the topaz granites are more likely to be melts from a fluid-rich amphibolite facies middle crust rather than a dry granulite lower crust.

The Cornish granites, like the Himalayan leucogranites, show a wide range in mineralogy, composition, and grain size, so the G1–G5 distinctions are not always clear cut. Muscovite, biotite, tourmaline, and lepidolite/zinnwaldite lithium micas are variable across individual plutons with minor phases such as garnet, cordierite, and andalusite also present. This suggests that all the surface plutons originated from a common source and are likely to be linked at depth, a proposal first made by De La Beche (1839) and supported by gravity studies of Bott et al. (1958, 1970) and Watts et al. (2024).

U-Pb and $^{40}Ar/^{39}Ar$ Ages

Dating the magmatic or intrusion ages of S-type granites is problematic due to high U concentrations, a paucity of zircon, and the likelihood of recycling of older zircon grains from sedimentary protoliths. Rb-Sr methods are unsuitable due to resetting during metamorphism or fluid fluxing. Ar-Ar methods only date cooling through the closure temperature of the minerals dated (e.g.: 300–350 °C for muscovite, biotite). Chen et al. (1993) presented concordant U-Pb monazite ages ranging from 293.1 ± 1.3 Ma (Carnmenellis) to 274.5 ± 1.4 Ma (Land's End) suggesting that the batholith was constructed over at least 20 m.y. (Fig. 2). Chesley et al. (1993) also presented U-Pb ages spanning the period 300 Ma to ca. 275 Ma (Bodmin Moor 291.4 ± 0.8 Ma; Carnmenellis 293.7 ± 0.6 Ma) with no systematic age trend along the batholith.

Zircon dating using laser ablation–inductively coupled plasma–mass spectrometry (LA-ICPMS) and isotope dilution–thermal ionization mass spectrometry (ID-TIMS) techniques of the Crownhill stock SW of Dartmoor yielded U-Pb ages from zircon cores of 288.9 ± 5 Ma and 286.4 ± 5 Ma,

while zircon rims from the same grains yielded ages of 277.74 ± 0.33 Ma and 278.35 ± 0.35 Ma (Smith et al., 2019). The Crownhill stock is the only pluton composed of two-mica, biotite, and tourmaline granites in the same intrusion. Zircon rims crystallized during the second phase of magmatism, probably linked to the biotite and tourmaline granites of Dartmoor and St Austell (Smith et al., 2019). In the greisen veins, cassiterite usually crystallizes with tourmaline, topaz, and Li-mica from exsolved magmatic-hydrothermal fluids, so the ages of zircon rims are thought to be synchronous with the Sn-mineralization. Neace et al. (2016) dated zircons using LA-ICP-MS that were consistently 20 m.y. older than previously established emplacement ages, a discrepancy that has been attributed to inherited zircons (Neace et al., 2016; Smith et al., 2019). Also noteworthy are the $^{40}Ar/^{39}Ar$ ages of associated lamprophyre dikes around the granites. These ages span 293.6–285.4 Ma, and overlap entirely with magmatic ages of the granites (Dupuis et al., 2015). The implication is that mantle-derived lamprophyres represent the surface expression of a wider magmatic underplating that would have provided additional heat input into the lower or middle crust that was ultimately responsible for the formation of the Cornubian granites.

Host-Rock Relations and Contact Metamorphism

The host rocks around the Land's End, Tregonning, and Carnmenellis granites are mudstones and mafic igneous rocks of the Devonian Mylor Slate Formation. The granites truncate folds, cleavages, and faults in the host rocks that formed during Variscan convergence and subsequent ductile, early post-Variscan extension, and are themselves cut by faults developed during later post-Variscan extension (Shail and Wilkinson, 1994; Alexander and Shail, 1995, 1996; Shail and Leveridge, 2009; Hughes et al., 2009). The Cornubian granites were, therefore, generated and emplaced in a post-orogenic extensional tectonic regime (Shail et al., 2003). A spectacular low-pressure, high-temperature contact metamorphic aureole is exposed in the 7-km-long St Just aureole, cropping out from Cape Cornwall to Portheras Cove on the north coast of the Land's End peninsula, and around the Tregonning granite on the south coast. Aureole rocks include both metapelite (cordierite + biotite + chlorite ± andalusite "spotted slates"), calc-silicates, and meta-basic cordierite + anthophyllite hornfels, all well exposed around Cape Cornwall at Kenidjack cliffs and Botallack (Tilley, 1935; Pownall et al., 2012). P-T modeling using THERMOCALC and pseudosection construction shows that contact metamorphism around the Land's End granite occurred at ~615 ± 50 °C and low pressures of ~150 ± 100 MPa (Pownall et al., 2012). This suggests that the top of the Land's End granite intrusions reached very shallow depths of ~2–5 km.

Mineralization

The Early Permian Cornubian high heat-producing granites are responsible for the formation of one of the classic polymetallic mining districts of the world. Historically, the district has produced mainly Sn and Cu, although other metals such as Fe, As, Pb, Zn, W, U, and Ag have also been extracted (Alderton, 1993). Mineralization in the granite is related to the exsolution of voluminous magmatic-hydrothermal fluids and their migration through faults and joints in the granite and host rocks (Jackson et al., 1989). Sn, Cu, W, and Zn are concentrated in the western part of the batholith from Cligga Head to Land's End (Fig. 1), whereas As, Fe, Pb, Ag, and Ba are concentrated mainly in the eastern part (WillisRichards and Jackson, 1989). Both Sn (cassiterite) and W (wolframite) are concentrated around the granite margins and occur within greisen veins and lodes emanating

from the granite and extending out into the country rock. Unusually, Cu is associated with Sn mineralization throughout Cornwall (Shail et al., 2003; Sillitoe and Lehmann, 2022). Greisen veins typically trend parallel to the axis of the batholith (WSW-ENE), whereas the epithermal Pb, Zn, and fluorite (and Ag, Ba) mineralization is associated with later crosscutting fractures ("cross-course veins") that strike at a high angle to the trend of the batholith (Willis-Richards and Jackson, 1989) and are related to the migration of basinal brines into the basement during the Triassic (e.g., Scrivener et al., 1994). Similar granites and styles of mineralization are also evident elsewhere along the Variscan orogenic belt, notably in Spain, Portugal, France, and the Czech Republic in Europe (Jacob et al., 2021), and also in New Brunswick– Newfoundland, Canada. In Europe these granites are mainly Carboniferous and are older than the SW England granites (Janousek and Zák, 2015). Presently the St Austell district remains a major producer of kaolinite (china clay) for the ceramics industry.

The source rock of the Cornish granites is sedimentary, comprising a significant component of black shale or pelitic equivalent, in common with many peraluminous granites. The actual source is unlikely to be the Mylor Slate Formation, exposed at the surface, because epsilon Nd values are significantly more negative than those of the plutons. However, on the basis of a time of removal from a depleted mantle source (T_{DM}) model age of 1.3–1.8 Ga (Darbyshire and Shepherd, 1994), the protolith is likely to be a Proterozoic shale-greywacke that remains buried at deeper structural levels. There is no surface expression of high-grade regional metamorphism as seen along the Himalaya (Searle et al., 1997, 2009). We speculate there must be a thick migmatite zone in the middle crust and that regional pelitic-psammitic metamorphic rocks that form the source for the granites are present, but remain buried and unexposed.

There is a link between the temperature of melting and granite prospectivity for tin and tungsten. Simons et al. (2017) have demonstrated that tungsten mineralization is more strongly associated with the earlier G1 (two-mica) and G2 (muscovite) granites that formed from lower-temperature muscovitedominated partial melting, since muscovite can accommodate trace contents of W within its lattice. In contrast the later, higher-temperature, biotite-dominated partial melting and differentiation was more strongly associated with tin mineralization due to derivation of Sn from biotite and Fe-Ti-oxides, as well as much higher boron contents resulting in tourmaline-dominated lode systems (Simons et al., 2017).

The muscovite and biotite dehydration melting reactions released borosilicate-rich fluids, which may have caused replacement of biotite by tourmaline, precipitation of cassiterite, and tin mineralization. Wolframite is the earliest mineralization phase (as seen at Cligga Head and Hemerdon mine) suggesting that tungsten was liberated from the source during the early phase of magmatism, whereas cassiterite is closely associated with tourmaline and fluorite, and usually precipitates as fluids cool (Romer and Kroner, 2016). Ar-Ar muscovite ages of ca. 290–270 Ma from graniterelated mineralized zones overlap with the U-Pb monazite ages, whereas later cross-course mineralization ages, from U-Pb uraninite, Rb-Sr, and Sm-Nd dating, are younger at ca. 236–206 Ma (see Shail et al., 2014).

Lamprophyre Dikes

In many orogenic belts A-type granites can be spatially and temporally related to late orogenic or post-orogenic mantle-derived alkali lamprophyres. In SW England, biotite and tourmaline granites were intruded coevally with lamprophyres (Dupuis et al., 2015, 2016; Dijkstra and Hatch, 2018). From the presence of synchronous lamprophyre dikes around the granites it is inferred that melting was driven by intrusion of mantle-derived mafic rocks into the lower crust. Lamprophyres are silica undersaturated, ultrapotassic mafic igneous rocks that have phenocrysts of amphibole, biotite, or phlogopite mica, and occur as dikes, sometimes associated with intrusive syenites and syeno-granites. They have alkalic compositions with high K, Na, Ba, Cs, Rb, and are derived from deep melting in the mantle, and low degrees of anatexis. Minettes (biotite, orthoclase-bearing lamprophyres; K-feldspar > plagioclase), kersantites (biotite, plagioclase; plagioclase > K-feldspar), vogesites (hornblende, orthoclase), and spessartites (hornblende, plagioclase) all form part of the lamprophyre suite. In SW England minettes are dominant with occasional kersantites (Dijkstra and Hatch, 2018). Lamprophyres have enriched light REE and large ion lithophile element concentrations, and depleted heavy REE suggesting a deep mantle garnet lherzolite source combined with metasomatic fluids. The lamprophyres in Devon and Cornwall are usually interpreted as representing mantle partial melting in response to post-collisional lithospheric extension, with possible mantle delamination or slab detachment (e.g., Dupuis et al., 2016).

3. GRANITE MODELS

The earliest studies of the SW England granites, conducted mainly by De la Beche (1839) and Ussher (1892), surmised that all the granites formed a single granite mass of roughly the same age. During the 1940s and 1950s, debate was split between those advocating differentiation (the "magmatists") and those who thought the granites resulted from metamorphism and anatexis (the "transformists")—the so-called "Granite controversy" of H.H. Read (1948). Brammall and Harwood (1932) were the first to develop a petrogenetic scheme based on partial melting of a metasedimentary source, and also recognized the importance of volatiles, particularly B, F, and H_2O. The original "Dartmoor model" lacked the complexities of the Liand F-rich granites seen around St Austell.

St Austell Model

A subsequent model for the shape and composition of the Cornubian granite was derived mainly from studies around the St Austell granite (Exley, 1958; Exley and Stone, 1982; Hill and Manning, 1987). This model (Fig. 3A) shows a series of compositionally distinct nested plutons all derived from fractionation of a biotite granite. Manning et al. (1996) described four main granite types from the St Austell pluton. The dominant lithology is biotite granite forming 70% of the outcrop (Qtz-Kfs-Pl-Bt-Ms) with late magmatic tourmaline associated with biotite and microperthite, and occasional large corroded cordierite. Accessory minerals include monazite, uraninite, rutile, and zircon. U-Pb zircon ages are 280.7–278.5 Ma (Chesley et al., 1993; Chen et al., 1993). Other mappable units are lithium-mica granites, tourmaline granite, and topaz granites. Microgranite dikes 1–30 m wide (known locally as "elvans") are oriented ENEWSW. Minor, late aplite dikes are composed of Qtz-Pl-Kfs-Li-mica with accessory tourmaline, topaz, and fluorite.

Floyd et al. (1993) summarized the early St Austell model and described the internal composition and zonation of the granite (Fig. 3A). Six major granite types (types A to F) were proposed of which Type B coarsegrained megacrystic biotite granite forms over 80% of the suite (Dartmoor, St Austell, Land's End granites). Type D megacrystic lithium mica and tourmaline granites and Type E lithium mica (lepidolite, zinnwaldite) granites are mostly confined to the St Austell and Tregonning granites, as well as locally along the northern margin of Dartmoor (e.g., Meldon aplite). Type F is the fluorite granites associated with late pegmatite and aplite veining. A combination of late magmatic-hydrothermal fluid flow and ingress from meteoric water has resulted in widespread kaolinization (china clay) and the breakdown of feldspar to clay minerals (Bristow, 1993). Tourmaline greisen veins within the granite have mostly withstood kaolinization processes.

1980s Model

With increasing geochemical and isotopic data another model, termed the "1980s model" (Fig. 3B), proposed that the Cornish granites were formed by melting of lower crust granulite facies meta-sedimentary rocks by heat derived from the mantle, and subsequent assimilation of upper crustal rocks (Floyd et al., 1993). Immobile trace element data, mainly Nb, Y, and Zr, together with high Rb, Ba, Zr, and Sn, as well as high radiogenic element (U, Th) contents indicate that the granites were derived from an evolved source, and not fractionated from a more basic magma, such as the Andean granites (see Floyd et al., 1993). Relatively high $^{87}Sr/^{86}Sr$ ratios (0.7095–0.7140) and Pb isotopes suggest a pelitic sedimentary source (Darbyshire and Shepherd, 1994). Occasional xenoliths containing garnet, sillimanite, andalusite, and cordierite confirm a likely peraluminous source (Stimac et al., 1995), although regional metamorphic rocks that could be source rocks are not exposed anywhere in SW England. Differentiation of lithium mica granites and topaz granites with increasing degrees of volatile saturation accompanied the mineralized veins. Most of the granites were thought to be either diapirs rising from a regional batholith at depth, or laccoliths, fed by dikes. They have uneven cupolas associated with a prominent contact metamorphic aureole, best exposed around the St Just coastline along the upper contact of the Land's End granite (Pownall et al., 2012). The older biotite granites are enclosed in later younger granites.

Taylor (2007) Model

Taylor (2007) carried out gravity modeling of the Dartmoor, Bodmin, and St Austell plutons and suggested that, unlike the Bott et al. (1958) batholith model, the deepest parts (~10 km) were evident along the steep southern margin, with a northerly directed flow. The Carnmenellis pluton was thought to have a centrally located deep feeder structure. Following the trend of interpreting granite emplacement as sill-like laccoliths fed from below by narrow, vertical conduits (e.g., Petford et al., 1993; Cruden, 1998), Taylor (2007) proposed that, at least for the Dartmoor granite, a steep southerly conduit (from ~20 km to 10 km depth) passed up into a horizontal northern extension. The other granites, however, do not show any steep gravity anomaly and the reduced model thicknesses do not accord with recent deep geothermal drilling east of the Carnmenellis granite where granite is proven to a true vertical depth of 5.058 km (Reinecker et al., 2021; Farndale and

Law, 2022). NNESSW and NW-SE lineations are shown on AMS (anisotropy of magnetic susceptibility) maps and inferred to represent extensional flow directions during the final emplacement process (Bouchez et al., 2006; Kratinová et al., 2010).

4. FIELD RELATIONSHIPS

Land's End Granite

The peraluminous Land's End biotite granite, with U-Pb monazite ages spanning 277 Ma (Zennor lobe) to 274.5 Ma (St Buryan lobe; Chen et al., 1993), occupies most of the Land's End peninsula and covers an area of ~190 km^2 (Shail et al., 2014). The older biotite granite sheets, with coarse-grained K-feldspar megacrysts up to 10 cm long, are enclosed by the younger tourmaline-rich granites, with uncommon euhedral cordierite. Mapping and petrology show that the Land's End pluton is a single, possibly composite intrusion, with all granites considered to have evolved by fractional crystallization from a common crustal source. Petrological studies indicate that the tourmaline granites evolved from fractionated lithium-siderophyllite granites (Müller et al., 2006). The upper parts of the plutons show magmatic and hydrothermal processes with banded leucogranites, aplites, and pegmatites indicating boron-rich hydrothermal fluids ponding along the uppermost contacts. Tourmaline concentration varies from sparse in early biotite granites to >50% in quartz + tourmaline schorl rocks. The upper contacts are usually abrupt and show intrusive relationships with the surrounding Mylor Slate Formation (Devonian), which has been affected by contact metamorphism. Detailed structural mapping shows that the granite intruded after ductile D3 deformation, the latest Carboniferous–Early Permian regional extension that followed Carboniferous contraction (Shail and Wilkinson, 1994; Alexander and Shail, 1995, 1996; Hughes et al., 2009; Alexander et al., 2019).

The upper contact of the Land's End granite is well exposed along the coastal sections from Cape Cornwall to Pendeen Watch (Fig. 4), and eastward toward Bosigran, Great Zawn, and Porthmeor Cove, and farther east to Zennor and St Ives. The metamorphic aureole rocks include cordierite + biotite + chlorite ± andalusite "spotted slates," and cordierite + anthophyllite meta-igneous rocks (Pownall et al., 2012). Dikes of leucogranites and pegmatites emanate from the upper margin of the Land's End granite into the country rocks (killas) and are associated with Sn, W, Cu, and As mineralization. Tin mining was first recorded in the Kenidjack region in 1502 and underground shafts were sunk at least by the 1780s. The Geevor (North Levant) tin mine was operational from 1911 to 1990 with over 135 km of tunneling both in the granite onshore and the killas offshore. The Botallack mine (Fig. 5A), operational from ca. 1550 to 1893, produced tin, copper, and arsenic from an underground network of shafts extending more than 400 m offshore and 500 m below sea level (Shail et al., 2014).

Cape Cornwall

The northern margin of the Land's End granite is well exposed at Priest's Cove and Porth Ledden, on either side of Cape Cornwall (Fig. 4). At Priest's Cove, the granite contact is partly mineralized along a fault (Saveall's lode). The granite contact abruptly cuts cordieritebearing metapelites

displaying folds and foliations developed during Variscan (D1 and D2) and post-Variscan (D3) deformation (Hughes et al., 2009). At Porth Ledden the granite contact is sharp and dips northward at 30°–40° (Fig. 5B). Quartz + tourmaline rocks are magmatic-hydrothermal in origin and crop out along the upper contact of the granite, representing the final magmatic phase (Müller et al., 2006). Pegmatites and aplites are also present, the result of the exsolution of magmatic-hydrothermal fluids along the upper margins of the cupolas.Cordierite-bearing spotted hornfels are present around the granite along the length of the St Just contact aureole.

The best exposures of the upper parts of the Land's End granite and its contact metamorphic aureole are the cliff sections from Kenidjack to the Crowns at Botallack (Pownall et al., 2012). The aureole rocks are metapelites derived from the Devonian Mylor Slate Formation and metabasalts, which include concordant basic sills and pillow lavas (Tilley, 1935; Pownall et al., 2012). Characteristic minerals in the hornfels are andalusite, biotite, cordierite, anthophyllite, ilmenite, and quartz. Uncommon calc-silicate skarns occur discordantly within the hornfels. Blue-gray cordierites form large spherical poikiloblasts up to 5 cm that have weathered out from the matrix. Brown-gray anthophyllite (orthoamphibole) occurs as needles within a matrix of biotite, plagioclase, and quartz. Uncommon sapphire has also been described from the Priest's Cove area (Floyd et al., 1993). Foliation in the host rocks is cut by the granite, which contains a few stoped blocks of hornfels around the margin. Quartz + tourmaline rock, interpreted as the final magmatic-hydrothermal fraction, crops out along the upper granite contact at Porth Ledden. Figure 6 is a geological cross section showing the field relationships around the top of the Land's End granite and the metamorphic aureole at Kenidjack. Cordierite + anthophyllite metabasalts are present, with cordierite-bearing metapelites above a gentle northerly dipping shallow granite contact. Mineral (Sn, W, Cu) lodes are related to late fluid pathways formed by hydraulic fracturing along faults and late joint sets.

Great Zawn, Bosigran

At Great Zawn (Fig. 7), west of Porthmeor Cove, the granite is connected to the main Land's End pluton, and was emplaced into a coarse-grained clinopyroxene-bearing metagabbro hosted by the Mylor Slate Formation metapelites. The granite contacts are sharp with several small tourmaline-rich granite dikes radiating outward to the northeast, toward Porthmeor Cove. North of Bosigran, the cliffs at Gala Rocks also show the contact of the Land's End granite with the hornfelsin the Mylor Slate Formation (C. Jurkowski, 2022, personal commun.). Numerous xenoliths along the granite margin show a variety of orientations and attest to a passive intrusion. At Wicca Pool, two large dikes composed of medium-grained biotite granite trend ENEWSW and dip to the SSE. Crosscutting relationships show at least two sets of leucogranite dikes emanating from the Land's End granite into the country rock.

Porthmeor Cove

The Porthmeor Cove area shows coastal outcrops of two satellite stocks composed of biotite + tourmaline granite (Stone and Exley, 1984; Pownall et al., 2012) intruded into theMylor Slate Formation, which has been metamorphosed to hornfels. The roof complex of the southern cupola comprises a banded leucogranite-pegmatite sequence structurally above the main biotite megacrystic granite (Fig. 5C). The upper cupola shows a sharp contact with metapelites of the contact aureole, and a prominent pegmatite layer along the granite margin. A network of fine-grained aplite sills crosscut structures in the country rock, both metapelites and metagabbros. Several generations of tourmaline-rich granite dikes radiate toward the NE toward Porthmeor, and one coarse-grained dike has offset an earlier fine-grained leucogranite sill by 1.5 m (Fig. 5D). Vertical tourmaline + quartz veins developed toward the top of the granite cupola. These late veins are also known to host Sn mineralization in the form of cassiterite. Numerous small xenoliths of the adjacent Mylor Slate Formation occur around the cupola margins.

Tregonning Granite

The Tregonning (Godolphin) granite is a fineto medium-grained peraluminous lithiummica (zinnwaldite, lepidolite) topaz granite stock (G5 granite) between the Land's End and Carnmenellis plutons (Stone, 1975, 1992; Exley and Stone, 1982; Breiter et al., 2018; Pownall et al., 2012). The Li-mica granite intruded the older biotite granite (Stone, 1975). The pluton has outward sloping western (Praa Sands) and eastern (Trequen) margins, and a warped but generally flat-lying upper contact (Fig. 8A). At Megiliggar Rocks along the eastern margin, three or four leucogranite sills extend horizontally east, intruding metapelites of the Mylor Slate Formation, which show andalusite and cordierite-bearing hornfels (Fig. 8B). Up to 3 mod% topaz occurs in lithium mica + muscovite/phengite + plagioclase (albite) + quartz pegmatite-aplite sheets and dikes that intrude into the Mylor Slate Formation hornfels. K-feldspar phenocrysts are uncommon, and quartz and schorl tourmaline are present, but restricted to local vugs and veins. The roof complex of the Tregonning granite is well exposed along the coast from Praa Sands, through Rinsey Cove to Megiliggar. At Rinsey Cove, the granite contact steps across the horizontal S3 cleavage in the country rocks. Several xenoliths are enclosed in granite and may provide evidence of stoping and subsidence (Floyd et al., 1993). The lithium mica and topaz granites show differentiation to fine grained leucogranite and banded pegmatiteaplite, with horizontal sills emanating from the top of the Tregonning granite into the Mylor Slate Formation, which shows contact metamorphism in the form of cordierite and andalusite hornfels.

Megiliggar Rocks

The granite sills at Megiliggar Rocks consist of banded aplite and pegmatite sheets (Figs. 9A and 9B) emanating from the main Tregonning granite, which has been offset by a late fault (Fig. 8). In comparison with other Cornubian granites, they are rich in Li, F, Sn, W, Nb, Ta, and U, and poor in Fe, Mg, Ca, Sr, Th, Zr, and REE (Breiter et al., 2018). Differentiation into a Li-Na-F-rich portion and a B-K-rich portion determines whether lepidolite/zinnwaldite or tourmaline crystallize from the melt (Breiter et al., 2018). Hydrothermal fracturing of fluid and volatile rich magmas caused escape upward into pegmatites and differentiated aplite dikes. Sn and W mineralization is concentrated in

the late veins and dikes. Occasional stoped blocks of slates are enclosed in the late granites (Fig. 9C). Banded pegmatite-aplite sills (Fig. 9D) contain cassiterite, Mn-rich apatite, columbite-tantalite, uraninite, and arsenopyrite, as well as rare wolframite (Simons et al., 2016; Breiter et al., 2018). Andalusiteand cordierite-bearing hornfels occur around the granite margins at Rinsey Cove and Megiliggar, similar to the contact metamorphic metapelitic hornfels seen along the north coast of Land's End.

Cligga Head

Cligga Head is located along the north coast of Cornwall between Perranporth and St Agnes (Fig. 1) and exposes a small stock of porphyritic biotite granite ~600 m long and intruded into metasedimentary rocks that have been affected by contact metamorphism and mineralization (Moore and Jackson, 1977; Fig. 10). The Cligga granite is most likely linked subsurface to the St Agnes granite 5 km to the SW, and extends an unknown distance offshore (Scrivener, 1903; Hall, 1971). The granite is composed of the assemblage: K-feldspar + plagioclase + quartz + muscovite + lithium micas (lepidolite, zinnwaldite), with accessory tourmaline and topaz. Country rocks are biotite + andalusite hornfels after Devonian slate. ENE-WSW–striking sheeted greisen veins intruding both granite and the country rocks indicate important Sn-W, and Cu-mineralized fluids, and numerous adits and shafts can be seen in the cliffs around Cligga Head (Fig. 11A). The granite is cut by numerous greisen-bordered veins, aligned ENE-WSW, and dipping ~70°–80° NNW (Figs. 11B and 11C). The greisen veins consist of quartz and mica (muscovite and lithium mica) enriched in Fe, Ca, F, B, Li, Mn, Rb, Sn, W, and Zn (Hall, 1971). Cassiterite, wolframite, and stannite show enrichment of tin and tungsten in the greisen veins, while copper, zinc, and arsenic are abundant in the unaltered granite. Vertical or steeply dipping NE-SW–oriented microgranite or rhyolite sheets (elvans) contain disseminated chalcopyrite mineralization. A prominent set of NNW-SSE–oriented "cross-course" veins, some showing Pb-Zn-Ag-fluorite mineralization, cut the granite (Scrivener et al., 1994; Shail et al., 2014). Cligga Head was the site of extensive mining during WW2 as a strategically important tungsten mine. Many copper-stained boulders are visible at low tide in Hanover Cove, 400 m south of Cligga Head (Fig. 11D). Tapster and Bright (2020) dated cassiterite from Cligga Head using chemical abrasion ID-TIMS U-Pb dating of zircon at 285.16 ± 0.1 Ma, slightly younger than the Carnmenellis granite, but older than the main Land's End granite. A later crosscutting rhyolite dike was dated at 283.21 ± 0.34 Ma (Tapster and Bright, 2020).

Carnmenellis Granite

The Carmenellis pluton, covering an area of ~130 km^2, is a highly evolved peraluminous leucogranite that lies adjacent to the most extensive mineralized lodes along the Camborne-Redruth zone (Fig. 1). The lodes are aligned ENE-WSW, dip steeply, and are hosted by the granite and the country rocks. Despite early mapping that distinguished various granites on the basis of grain size, all varieties are mineralogically and chemically similar, being biotite–muscovite– K-feldspar megacrystic granite typical of early granites of the batholith (Exley and Stone, 1982). Lithium mica–albite–topaz granites comprise a minor component, and are similar to those described from the Tregonning granite. Charoy (1986) suggested that the Carnmenellis granite resulted from partial melting of a cordierite-sillimanite-spinel pelite with a high water content of ~4%. Extensive hydrothermal circulation has resulted in localized kaolinization of the granite. Rb-Sr dating of a Sn-W vein from South Crofty Mine

(269 ± 4 Ma) is considerably younger than the age of the granite (290–280 Ma) suggesting than fluid circulation may have outlasted magmatism by >10 m.y. (Darbyshire and Shepherd, 1985). U-Pb zircon core dating constrains the early magmatic age of the Carnmenellis granite at 293.1 ± 1.3 Ma and 288.9 ± 5 Ma and 286.4 ± 5 Ma (Chen et al., 1993).

St Austell Granite

The St Austell pluton, covering ~85 km^2 (Fig. 12), is the most varied of all the Cornish granites with lithologies ranging from biotitegranite, through to fine-grained lithium mica granite, to quartz + tourmaline schorl granite, such as exposed at Luxulyan quarry and Roche Rock (Manning et al., 1996). Late topaz granites and fluorite granites form a north-south belt (Nanpean topaz granite) separating two biotite K-feldspar megacrystic granites (Fig. 12). Topaz-rich lithium mica granite contains both wolframite and cassiterite, and lacks significant tourmaline. Both lithium mica granites and topaz granites are exposed in Tregargus quarry, St Stephen, where they intrude all lithologies except the late-stage rhyolite porphyry dikes called elvans (Manning and Exley, 1984; Manning et al., 1996). Topaz granites are thought to have intruded along the roof complex of the St Austell granite pluton (Floyd et al., 1993). These rocks span the magmatic to hydrothermal boundary in the crystallization-cooling history. Luxulyanite is an unusual granite containing coarse, red, K-feldspar megacrysts, biotite and minor plagioclase with rare muscovite, apatite, topaz, andalusite, and fluorite. Extensive boron-rich fluids have resulted in black tourmaline replacement, which together with red K-feldspar characterizes luxulyanite. The luxulyanite occurs in near vertical sheets striking ENE-WSW, parallel to the main mineralization lodes (Floyd et al., 1993). Regional hydrothermal alteration has resulted in extensive kaolinization during which the feldspars have almost completely been replaced by clay minerals leaving the less altered quartz + tourmaline veins standing proud.

Bodmin Moor Granite

The Bodmin Moor granite, covering an area of ~190 km^2, is one of the oldest plutons of the Cornubian batholith, along with Carnmenellis and the Isles of Scilly (300–288 Ma; Chen et al., 1993; Chesley et al., 1993). It is a homogeneous coarse-grained biotite granite and contains ~1% tourmaline (Stone, 2000; Chappell and Hine, 2006). In some places, alignment of feldspar megacrysts define igneous flow banding with a north-south strike (Floyd et al., 1993). AMS fabrics are compatible with NNW-SSE stretch of the crystallizing granite and reflect both magmatic-state and solid-state deformation (Bouchez et al., 2006). Zircon cores from the Bodmin granite yielded ages of 291.4 ± 0.8 Ma (Chesley et al., 1993). A single intrusive phase of coarse-grained megacrystic biotite granite is present throughout with rare, crosscutting, late quartz-feldspar porphyry (elvans) dikes up to 10 m thick, striking ENEWSW (Exley, 1996).

Dartmoor Granite

The Dartmoor granite is the largest granite pluton in SW England, covering an area of >600 km2. U-Pb monazite dating suggests an intrusive age of 286–281 Ma and 279.5 ± 1.0 Ma (Ches- ley et al., 1993). The outcrops around Hay Torconsist of megacrystic biotite syenogranites with an

earlier, coarse-grained variety overlying a lower, fine-grained granite (Brammall and Harwood, 1932). Some K-feldspar megacrysts are up to 12 cm long and in places show a weak magmatic alignment. Clemens et al. (2021) suggested that the Dartmoor granite evolved from high-temperature, fluid-present biotite-break- down melt reactions. Isotopic heterogeneities suggest that the magma did not homogenize by mixing or convection. Uncommon xenoliths include biotite, cordierite, corundum, and aluminosilicate hornfels from the contact metamorphic aureole (Stimac et al., 1995) and may represent either high-temperature deeper parts of the aureole, or have a restitic origin from a shallow melt source.

Very rare hornblende-bearing meta-igneous enclaves reported by Brammall and Harwood (1932) and Stone (1995) are thought to be related to the Permian lamprophyres or high-K basalts of the adjacent Exeter Volcanic Rocks (Stimac et al., 1995). Several generations of tourmaline growth include magmatic and metasomatic varieties and tourmaline schorl "stars" in quartz + tourmaline veins and enclaves (Duchoslav et al., 2017). The Dartmoor granite, however, generally lacks the Li-mica and topaz granites seen around Tregonning and St Austell. An exception is the 20 m thick Meldon aplite dike intruded into the Carboniferous (Namurian) Culm sedimentary rocks ∼1–1.5 km north of the northern contact of the Dartmoor granite. The Meldon dike consists of albite + quartz + lepidolite + topaz + fluorite, and contains a wide variety of unusual lithium-,boron-, beryllium-, fluorine-, and rare earth element minerals (Edmonds et al., 1968; Floyd et al., 1993). The Meldon aplite dike is similar to the aplite-pegmatites and the lithium-mica and topaz granites seen around the roof complex of the Tregonning granite at Rinsey Cove and Megiliggar Rocks.

A major tungsten-tin deposit is present at Drakelands mine in the Hemerdon area, 12 km NE of Plymouth, where a small stock of muscovite granite lies adjacent to the main Dartmoor granite (Leveridge et al., 2002). The Hemerdon stock comprises a NNE-striking dike intruding the Devonian slates and metavolcanic rocks and is cut by a prominent set of NW-SE–striking faults and fractures. Similar to the Cligga Head deposits, mineralization is associated with NW-dipping greisen veins consisting of quartz + ferberite (wolframite) + cassiterite. Large china clay pits around Hemerdon show that the sur-rounding granite body is strongly kaolinized.

5. NEW MODEL FOR THE CORNUBIAN GRANITES

Figure 13 shows a new model for the Cornubian granite batholith, based on recent work carried out on the nubian granite batholith, based on recent work carried out on the Land's End, Tregonning, and Carnmenellis granite plutons. The shapes of the upper cupolas of the granites are constrained from field mapping. Present-day exposure shows only the upper 1–3 km of structural depth, and suggests that the granites were intruded up to very shallow levels of the crust. The lower parts of the model are partially constrained from gravity data (Bott et al., 1958; Willis-Richards and Jackson, 1989; Watts et al., 2024). The shape of the granites is modeled as upward flaring conduits feeding upper crust laccolithic intrusions that bulge upward toward the surface as a result of magmatic injection and roof inflation (Part 2; Watts et al., 2024). The spots around the upper cupolas represent the contact metamorphic aureole, which includes metapelites (cordierite + biotite + chlorite ± andalusite "spotted slates"), and metabasalts (cordierite + anthophyllite hornfels), metamorphosed at low pressures of 150 ± 100 MPa (Pownall et al.,

2012), indicating the emplacement of adjacent granites to depths of only 2–5 km. New gravity modeling suggests steep-sided plutons passing down into a regionally linked melt zone (Part 2; Watts et al., 2024). The melt zone can only be inferred, but it must be a high-grade metamorphic or migmatite lithology that is not exposed at the surface.

Granites in SW England are at least 5 km thick from recent drilling data (Farndale and Law, 2022) and possibly up to ~10 km thick from gravity modeling (Part 2; Watts et al., 2024). Seismic surveys by Brooks et al. (1984) and Jones (1991) show two prominent reflectors R1 and R2 at depths of 7–8 km and 11–14 km, respectively. As the R1 seismic reflector appears to be within the lower part of the gravity-defined granite, it is not clear what this represents geologically. The precise nature of the base of the granite is debatable but we interpret the zone beneath ~10 km depth as representing a zone of sillimanite + muscovite ± cordierite + K-feldspar migmatite from which the granites separated and rose to higher level sheet-like bodies, fed by dikes. This structure, depth, and mode of emplacement is similar to that seen in petrologically similar leucogranites in the Himalaya, where the melt source zone is exposed (Searle et al., 2009). A third reflector R3, at a depth of 28–30 km, is interpreted as the Moho (Brooks et al., 1984). The lower crust, between the R2 and R3 reflectors is likely the Variscan basement composed of Proterozoic crust and probably granulite facies rocks. These hot, dry granulites are unlikely to be the melt source as far higher temperatures would be required to melt granulites than those implied for the SW England granites.

We interpret the feeder system as conduits and dikes that fed magma to the batholith from the mid-crust melting source zone (green area in Fig. 13). The mid-crust melt zone is modeled as ~5–7 km thick, between the R2 reflector and a poorly-defined zone at ~20 km depth, which separates a hydrous, weak, partially molten, upper amphibolite facies migmatite zone midcrust from a lower crust composed of dry, hightemperature granulite that has not been subjected to melting. The melt source for the granites (pelite, psammite) is thought to be Proterozoic in age, and not the Devonian Mylor Slate Formation into which the granites have intruded at the surface. The source is also inferred to be isotopically heterogeneous because not all lithologies can be ascribed to fractional crystallization (Simons et al., 2016, 2017; Clemens et al., 2021).

All the granites, including the early G1 two-mica granite (Carnmenellis; pink color on Fig. 13), the dominant G3-G4 biotite + tourmaline + K-feldspar megacrystic granite (Land's End, red color), and the G5 lithium mica + topaz granites (Tregonning; orange color) are thought to originate from a mid-crust upper amphibolite facies migmatite zone, capped by the R2 seismic reflector, which dips gently ENE from depths of ~12 km beneath Land's End to ~15 km depth beneath south Devon (Brooks et al., 1984; Jones, 1991). The granites are thought to have been derived from muscovite and biotite dehydration reactions at temperatures of ~700–800 °C and low pressures of (~300–600 MPa) from a dominantly pelitic or psammitic melt lithology in the mid-crust (Simons et al., 2016). The lithium mica and topaz granites and aplites at Tregonning are thought to originate from melting of a metapelite, or greywacke source similar to the two-mica and tourmaline granites, and not from the lower crust granulite zone, because of the lack of orthopyroxene and hornblende in the melt. We infer that the mid-crust between the R1 and R2 reflectors is composed of regional

Barrovian facies metamorphic rocks that are not exposed at the surface.

Mantle-derived lamprophyre dikes (minettes, kersantites) are spatially and temporally associ- ated with, and intruded simultaneously with the granites, but are sourced from a highly meta- somatized alkaline upper mantle. Basaltic and lamprophyric magmas are thought to have been underplated, and/or emplaced within the lower crust, bringing excess heat and volatiles to the magma source (Shail et al., 2003; Dupuis et al., 2015, 2016). The volume of granite in SW England requires an extra heat source apart from the main internally derived radioactive heating.

6. DISCUSSION

I-Type, S-Type, and A-Type Granite Classification

Of the many classification schemes that exist for granitic rocks one of the most relevant is the Iand S-type scheme, originally devised for the Lachlan Fold Belt in southeast Australia by Chappell and White (1974). In its simplest form the scheme implies that orogenic granites can be subdivided on the basis of whether their parental magmas were derived by partial melting of predominantly igneous (I-type) or sedimentary (S-type) source rock. In general, I-type granites tend to be higher temperature (>850–900 °C) hornblende melting, metaluminous, and typified by tonalitic (or quartz-dioritic) and granodioritic compositions, and require an extra source of heat (e.g., basaltic underplating, supra-subduction zone fluids). S-type granites are lower temperature (700–750 °C) muscovite or biotite melting, peraluminous, and have adamellitic (or quartz-monzonitic) to leucogranitic compositions. Also important from a metallogenic viewpoint is the fact that I-type granites tend to be more oxidized; i.e., they have a higher magmatic fO_2 than S-type granites, whose magmas were originally fairly reduced because of the presence of material such as carbon (graphite) in their source rocks.

Another classification of granites according to oxidation state was made initially by Ishihara (1977), who distinguished between reduced granite magmas (forming ilmenite-series granitoids) and more oxidized equivalents (forming magnetite-series granitoids). The metallogenic significance of this type of granite classification was also recognized by Ishihara (1977), who indicated that Sn-W deposits were preferentially associated with reduced ilmenite-series granitoids, whereas Cu-Mo-Au ores could be linked genetically to oxidized magnetite-series granitoids. Magnetite-series granitoids are equivalent to most I-types, whereas ilmenite-series granitoids encompass all S-types as well as the more reduced I-types. I-type granites typically are associated with Andean-type andesite-daciterhyolite volcanics, whereas S-type granites generally have no volcanic component. The Cornubian granites have very limited extrusive volcanic phases but are temporally and spatially associated with mantle-derived lamprophyres and high-K basalts. The Kingsand rhyolite in SE Cornwall is one of the few preserved extrusive volcanic phases associated with the granites (Leveridge et al., 2002).

A-type granites are anorogenic, or alkali granites, typically of appinitic composition, with a higher proportion of K-feldspar over plagioclase, and high concentrations of alkali elements, Zr, Nb, Y, Ce, etc. A-type granites are derived from high-temperature melting of granulite type rocks. However,

highly fractionated Iand S-type granites can overlap with A-type granites (Whalen et al., 1987). A-type granites are generally formed in intraplate or continental rift environments, and are frequently associated spatially and temporally with mantle-derived lamprophyres.

The Cornubian granites have many characteristics of ilmenite series S-type granites, including peraluminous compositions, K-feldspar, muscovite, cordierite, biotite, andalusite, sillimanite, tourmaline, topaz mineralogy, Sn-W mineralization, and abundant pegmatite-aplite diking. The source rocks are not seen, but are presumed to be mid-crustal amphibolite facies meta–pelitic-psammitic gneisses, or migmatites. The Cornubian granites are, however, more batholithic than Himalayan type granites, and have intruded to very shallow levels in the crust. The synchronous intrusion of lamprophyre dikes around the granites might suggest higher temperature melting with a significant mantle input. The Cornubian granites are not hornblende-bearing, magnetite series, I-types, and are not related to a subduction zone, either spatially or temporally. They were also formed 80–90 million years after formation and obduction of the Lizard ophiolite, after Carboniferous Variscan deformation of the Culm intraplate basin, and after the onset of post-convergence extension, so they are post-orogenic in origin.

Source and Depth of Melting

Exposed levels of the Land's End and Tregonning granites only show the shallow levels of emplacement (2–5 km depth maximum) into sedimentary rocks. The deeper levels of all Cornish granites are not exposed, so the in situ melting source region must be inferred from petrology, chemistry, and xenolith composition. Peraluminous Himalayan granites, also rich in tourmaline, biotite, muscovite, garnet, and cordierite, are emplaced as giant sill complexes, and are associated with a regional sillimanite + K-feldspar migmatite melt source region at mid-crustal depths (Searle et al., 2009). It is likely that the deeper, unexposed levels of the Cornubian crust similarly comprise regional Barrovian facies metamorphic rocks and migmatites. The composition of the lower crust is presumed to be granulite or amphibolite facies from rare enclaves in the granites with the assemblage: garnet + sillimanite + plagioclase + cordierite + spinel + quartz (Charoy, 1986; Stimac et al., 1995). These are thought to have a restitic origin, whereas the andalusite assemblages, without sillimanite, are probably thermally metamorphosed contact aureole rocks. Meta-igneous enclaves, comprising less than 1%, range from monzogranite to tonalite.

Lamprophyric dikes are widespread and were intruded between 295 Ma and 285 Ma (Dupuis et al., 2015, 2016), simultaneously with the granites (Smith et al., 2019). Lamprophyres are mantle-derived alkalic intrusive rocks associated with metasomatism and are genetically related to kimberlites and lamproites, derived from a garnet-bearing deep mantle source. They are commonly related to Snand W-bearing peraluminous granites such as the Cornish granites, and transferred fluids and heat-producing elements (K, Th) from the metasomatized upper mantle into the crust, promoting granite melting. Dijkstra and Hatch (2018) "mapped" a hidden terrane boundary running east-west across the middle of Dartmoor and north Bodmin Moor, based solely on Sr and Nd isotopes. They suggested that lamprophyres north of the line with epsilon Nd values of −1 to +1.6 differ from those south of the line, which are enriched in radiogenic Sr and have epsilon Nd

values of −3 to −3.5. However, it could equally be argued that all the lamprophyres show an increasing $^{87}Sr/^{86}Sr$ enrichment trend toward the south along a straight line (Dijkstra and Hatch, 2018; Fig. 1C). Epsilon Nd values are similar across the proposed boundary, and there is no evidence from surface geology of a suture zone in this locality. The suture zone is located south of the Lizard peninsula from the Lizard ophiolite running east along the English Channel and has been imaged on the British Institutions Reflection Profiling Syndicate seismic reflection profiles (SWAT—south-western approaches traverse) as a wide zone, ~8 km thick, dipping to the south (Le Gall, 1990; Alexander et al., 2019). The SW England granites and lamprophyres are all intruded into the lower, footwall plate, rather than above a subduction zone.

Emplacement Mechanisms

The source region of the Cornubian granites is unexposed, but is assumed to be a high-temperature migmatite zone where pervasive granite leucosomes form from melting at temperatures ~700–750 °C. Leucosomes eventually link to form melt pathways along shear zones or dike-sill complexes, as seen along parts of the Himalaya (Searle et al., 2009) and the Karakoram (Weinberg and Searle, 1998, 1999). Potential granite emplacement mechanisms include forceful diapirism and ballooning plutons (Weinberg and Podladkicov, 1994), diking (Petford et al., 1993; Reichardt and Weinberg, 2012), transtensional emplacement into fault zones (Hutton and Reavy, 1992), transpressional emplacement (D'Lemos et al., 1992; Brown and Solar, 1998), wall rock assimilation, laccoliths (Scaillet et al., 1995; Cruden, 1998), and wedge-shaped plutons (Cruden and Weinberg, 2018). Magma, once generated in the source region, can be transported to higher structural levels via fractures or shear zones (see Brown, 2007, 2013, for reviews). In general, plutons are thought to have been constructed incrementally as a result of cyclic melt extraction from the source (Brown, 2013). In Cornwall and Devon, only the highest structural levels are exposed, and thus, the melt source and feeder zone have to be inferred from geophysical data.

Comparison with Other Granite Batholiths

Few orogenic belts expose granite batholiths from top to bottom, but three examples are exceptional—the Patagonian batholith in Chile, the Baltoro Karakoram granite batholith in Pakistan, and the Himalayan leucogranites, and we use these examples to compare and infer the possible deep structure of SW England.

The Patagonian batholith in the Torres del Paine area, southern Chile, was formed by incremental injection of three biotiteand hornblende-bearing granite pulses, intruded as giant sills building a horizontal layered laccolith (Michel et al., 2008). These three sills, dated as 12.59 ± 0.02 Ma (oldest) to 12.50 ± 0.02 Ma (youngest), show that the 2-km-thick laccolith was built over 90 ± 40 k.y. from the top down, at a depth of only 2–3 km (0.7 ± 0.3 kbar). Relic orthopyroxene and olivine, and magmatic hornblende, indicate that the Torres del Paine granites are I-type granites, ultimately derived by melting from a gabbrodiorite source. This laccolith geometry appears to be very different from the classic Andean-type plutons farther north in northern Chile and Peru, but it shows that I-type granites can intrude as dike-fed laccoliths.

The second example comes from the classic Miocene S-type leucogranites of the Himalaya (Searle, 1999; Searle et al., 1997, 2003, 2009). The entire Himalayan crust is tilted northward so it possible to trace and map the whole crustal section from in situ melt source to high-level sill complex over a structural profile of at least 10–20 km. The melt zone is a thick mid-crust layer of sillimanite + K-feldspar migmatite showing in situ melting of garnet, tourmaline, muscovite ± cordierite leucosomes, with biotite + sillimanite + garnet ± cordierite restite (Searle, 1999). Wispy leucosomes converge into melt channels, which in turn feed higher level sills, fed from narrow dikes along the base (Searle et al., 1997, 2003, 2009). The highest levels of the granites show horizontal or gently north-dipping sills of leucogranite, bounded along the top by the South Tibetan Detachment (STD) normal fault, that was active during intrusion of the granite. The STD formed the roof fault of the southward extruding channel comprising high-grade metamorphic rocks, migmatites, and leucogranites (mid-crustal Channel Flow). The Himalayan granites have petrological similarities with the Cornubian granites in Devon and Cornwall, but exposure here does not extend far down beneath the upper cupolas. Major differences are the lack of mineralization in the Himalayan leucogranites, and a close association with in situ migmatization.

The third example comes from the giant (700 km long, 7–20 km wide) Baltoro batholith in the Karakoram of north Pakistan (Searle et al., 2010). Here the crust is also tilted to the north, revealing the full 10–20 km exposure of the Baltoro granites and their substrate, the Karakoram Metamorphic complex. The upper levels in the Baltoro granites comprise at least 5–10 km thickness of massive garnet, tourmaline, and muscovite monzogranite-leucogranite, spectacularly exposed in the Trango Towers and along almost 700 km strike length in northern Pakistan and northern Ladakh. The Miocene Baltoro granites crystallized between 20 Ma and 13 Ma (Searle et al., 2010) and were intruded into earlier biotite-hornblende bearing diorites and granodiorites (Hushe gneiss, K2 gneiss). The upper structural levels in the Masherbrum range show horizontal leucogranite sills up to 2–3 km thick, fed by dikes below. The upper (northern) contact of the Baltoro granite shows a classic sillimanite-andalusite hornfels ($P < 300$ MPa) contact metamorphic aureole, ~100–200 m wide, superimposed onto Carboniferous black slates. The deeper (southern) contact shows a wide migmatite melt zone crossed by numerous leucogranite dikes and sills emanating from a regional kyanite and sillimanite grade terrane. Post-collisional metamorphism lasted at least 37 m.y. and possibly as much as 50 m.y (Searle et al., 2010). The massive nature of the Baltoro granites has similarities with the Cornubian granites, but none of the melt zone or the Barrovian facies metamorphic rocks beneath are exposed in SW England. Further similarities with the Baltoro granites are the presence of synchronous lamprophyre dikes intruding around the granites in the Pakistan Karakoram and SW England. One major difference is the lack of mineralization in the Baltoro granites compared to the Cornubian granites. The Cornubian granites could also be compared closely with the Triassic S-type tin granites of peninsular Malaysia, in terms of magma volume, composition, and mineralization (Ng et al., 2015).

The batholitic nature of the Cornubian granites in unlike the structure of the Himalayan leucogranites (Searle, 1999; Searle et al., 1997, 2009), but is more akin to the large-scale Baltoro granites in the Karakoram (Searle et al., 2010). In both SW England and the Karakoram, granite melting was synchronous with intrusion of small volume lamprophyre dikes that suggest a

component of mantle-derived heat and volatiles from underplated alkaline magma. U-Pb zircon ages of the Cornubian granite show that these Permian magmas were intruded 80–90 m.y. after the obduction of the Lizard ophiolite northward onto the Avalonian continent (Mackay-Champion et al., 2024), which marks the beginning of the Variscan orogeny in SW England. The Cornubian granites are, therefore, post-orogenic and generated and emplaced in an Early Permian regional extensional tectonic setting (e.g., Shail and Alexander, 1997; Alexander et al., 2019), but whether slab detachment or lithospheric delamination contributed to partial melting is unclear (e.g., Dupuis et al., 2016). The Cornubian granites were also intruded along the downgoing plate (Avalonia) and cannot be compared directly to earlier, similar granites in Brittany, Spain, and Portugal on the opposing Armorican plate (Jacob et al., 2021).

7. CONCLUSIONS

We draw the following conclusions from this review of field, structural, petrological, and geophysical data of the Cornubian granites of SW England:

1) The Cornubian granites are crustal melt granites with mineralogy (Qtz + Kfs + Pl + Bt + tourmaline (Tur) + Ms ± Li-mica ± topaz) and peraluminous geochemistry consistent with sedimentary source rocks and S-type granites (Müller et al., 2006; Simons et al., 2016; Breiter et al., 2018; Clemens et al., 2021). They were intruded during the Permian, between 293 Ma and 274 Ma (U-Pb monazite dating; Chen et al., 1993; Chesley et al., 1993; Smith et al., 2019).

2) The Cornubian granites form a batholith over 250 km long with individual plutons rising from a common connected batholith at depth (see Part 2, Watts et al., 2024).

3) The melt source is likely to be a heterogeneous pelite-psammite from the lower part of the mid-crust, probably of Proterozoic age. The granites are intruded into the Devonian Mylor Slate Formation or the Carboniferous Culm sediments (Dartmoor) at the surface, but these rocks are unlikely to be the source rock at >8 km depth.

4) Petrology, peraluminous geochemistry, and similarities with Himalayan leucogranites suggest that the Cornubian granites were likely derived from a regional sillimanite grade metamorphic-migmatite metapelitic source, which is not exposed at the surface.

5) A contact metamorphic aureole, consisting of metapelites (cordierite + biotite + chlorite ± andalusite “spotted slates”), calc-silicates, and meta-basaltic cordierite + anthophyllite hornfels, was formed at temperatures of ∼615 °C and pressures less than 150 ± 100 MPa (Pownall et al., 2012) indicating that the granites arose from their mid-crust source and intruded upward to within ∼3 km of the surface.

6) The Cornubian granites were intruded synchronously with a suite of lamprophyre dikes that indicate coeval upper mantle melting and crustal melting (e.g., Stimac et al., 1995; Dupuis et al., 2015). The alkaline mantle melting and mafic underplating may have provided the extra heat required for melting such a large volume of granite.

7) Tin and tungsten mineralization is generally associated with greisen-bordered sheeted veins and lode systems that cut through the granite and continue into the host rocks. Mineralization processes range from late magmatic to hydrothermal. Tin and tungsten lodes

occur commonly around the upper margins of the granites, and copper is more common within the surrounding country rocks. Later Triassic epithermal "cross-course" mineralization (leadzinc) in the host rocks is associated with NNWSSE–striking steep veins that cut the granite and host rocks.

8) The Cornubian granites are post-orogenic and were intruded during the Early Permian, ~90 m.y. after the start of the Variscan orogeny and emplacement of the Lizard ophiolite in south Cornwall (Mackay-Champion et al., 2024). Variscan continental collision and structural inversion in the Carboniferous was followed by regional extension and lithospheric thinning during the latest Carboniferous–Early Permian that resulted in coeval mantle and crustal partial melting.

9) The Cornubian granites are most similar to the Baltoro granite batholith in the Pakistan Karakoram, where intrusion of a major S-type granite batholith was also concomitant with a suite of lamprophyre dikes. Although mineralogically similar to Miocene Himalayan leucogranites, the SW England granites were not intruded into sillimanite grade gneisses and migmatites at depth, but were intruded as diapirs or plutons rising from a common inter-connected source at depth.

ACKNOWLEDGMENTS

We are grateful to George Willment (Imerys British Lithium), Tobermory MacKay-Champion, Sam Hughes, Beth Simons, and Jens Andersen for field assistance and discussions, and thanks to Dave Sansom for drafting. Thanks to Chris Yeomans, Lucy Crane, and Hugo Heard (Cornish Lithium) for access to core samples. M.P. Searle gratefully acknowledges a Leverhulme Emeritus Fellowship. We thank Damian Nance and an anonymous reviewer for detailed and constructive comments and the science editor, Mihai Ducea, for helpful suggestions that improved the paper.

REFERENCES

Alderton, D., 1993, Mineralisation associated with the Cornubian granite batholith, *in* Pattrick, R., and Polya, R., eds., Mineralisation in the British Isles: New York, Chapman & Hall, p. 270–354.

Alexander, A.C., and Shail, R.K., 1995, Late Variscan structures on the coast between Perranporth and St Ives, Cornwall: Proceedings of the Ussher Society, v. 8, p. 398–404.

Alexander, A.C., and Shail, R.K., 1996, Late- to post-Variscan structures on the coast between Penzance and Pentewan, south Cornwall: Proceedings of the Ussher Society, v. 9, p. 72–78.

Alexander, A.C., Shail, R.K., and Leveridge, B.E., 2019, Late Paleozoic extensional reactivation of the RheicRhenohercynian suture zone in SW England, the English Channel and Western Approaches, *in* Wilson, R.W., Houseman, G.A., McCaffrey, K.J.W., Doré, A.G., and Buiter, S.J.H., eds., Fifty Years of the Wilson Cycle Concept in Plate Tectonics: Geological Society, London, Special Publication 470, p. 353–373, https://doi.org/10.1144/SP470.19.

Bonin, B., Janousek, V., and Moyen, J.-F., 2020, Chemical variation, modal composition and classification of granitoids, *in* Janoušek, V., Bonin, B., Collins, W.J., Farina, F., and Bowden, P., eds., Post-Archean Granitic Rocks: Petrogenetic Processes and Tectonic Environments: Geological

Society, London, Special Publication 491, p. 9–51, https://doi.org/10.1144/SP491-2019-138.

Bott, M.H.P., Day, A.A., and Masson-Smith, D., 1958, The Geological interpretation of Gravity and Magnetic surveys in Devon and Cornwall: Philosophical Transactions of Royal Society, v. 251, p. 161–191.

Bott, M.H.P., Holder, A.P., Long, R.E., and Lucas, A.L., 1970, Crustal structures beneath the granites of South West England, *in* Newell, G., and Rast, N., eds., Mechanism of Igneous Intrusion: Geological Journal, Special Issue (Liverpool, UK), v. 2, p. 93–102.

Bouchez, J.L., Ngeuma, T., Esteban, L., Sequirer, R., and Scrivener, R., 2006, The tourmaline-bearing granite pluton of Bodmin (Cornwall, UK): Magnetic fabric study and regional inference: Journal of the Geological Society, v. 163, p. 607–616, https://doi.org/10.1144/0016-764905-104.

Brammall, A., and Harwood, H.F., 1932, The Dartmoor granite: Their genetic relationships: Quarterly Journal of the Geological Society, v. 88, p. 171–237, https://doi.org/10.1144/GSL.JGS.1932.088.01-04.09.

Breiter, K., Durisova, J., Hrstka, T., Korbelova, Z., VasinovaGaliova, M., Müler, A., Simons, B., Shail, R.K., Williamson, B.J., and Davies, J.A., 2018, The transition from granite to banded aplite-pegmatite sheet complexes: An example from Megiliggar Rocks, Tregonning topaz granite, Cornwall: Lithos, v. 302–303, p. 370–388, https://doi.org/10.1016/j.lithos.2018.01.010.

Bristow, C.M., 1993, The genesis of the china clays of south-west England—A multistage story, *in* Murray, H.H., Bundy, W.M., and Harvey, C.C., eds., Kaolin Genesis and Utilization: Clay Minerals Society Special Publication 1, p. 171–203, https://doi.org/10.1346/CMS-SP-1.8.

British Geological Survey, 1982, Scilly Sheet 49 N 08 W Solid Geology, 1:250 000 UTM Series: Geological maps of the UK and continental shelf areas, British Geological Survey, v. 10.

Bromley, A.V., and Holl, J., 1986, Tin mineralisation in southwest England, *in* Willis, B.A., and Barley, R.W., eds., Mineral Processing at a Crossroads: Dordrecht, Netherlands, Martinus Nijhoff, NATO Series 117, p. 195–262, https://doi.org/10.1007/978-94-009-4476-3_8.

Brooks, M., Doody, J.J., and Al-Rawi, F., 1984, Major crustal reflectors beneath SW England: Journal of the Geological Society, v. 141, p. 97–103, https://doi.org/10.1144/gsjgs.141.1.0097.

Brown, M., 2007, Crustal melting and melt extraction, ascent and emplacement in orogens: Mechanisms and consequences: Journal of the Geological Society, v. 164, p. 709–730, https://doi.org/10.1144/0016-76492006-171.

Brown, M., 2013, Granite: From genesis to emplacement: Geological Society of America Bulletin, v. 125, p. 1079–1113, https://doi.org/10.1130/B30877.1. Brown, M., and Rushmer, T., 2006, Evolution and Differentiation of the Continental Crust: Cambridge, UK, Cambridge University Press, 562 p.

Brown, M., and Solar, G.S., 1998, Granite ascent and emplacement during contractional deformation in convergent orogens: Journal of Structural Geology, v. 20, p. 1365–1393, https://doi.org/10.1016/S0191-8141(98)00074-1.

Burov, E., Jaupart, C., and Guillou-Frottier, L., 2003, Ascent and emplacement of buoyant

magma bodies in brittleductile upper crust: Journal of Geophysical Research: Solid Earth, v. 108, no. B4, https://doi.org/10.1029/2002JB001904.

Chappell, B.W., and White, A.J.R., 1974, Two contrasting granite types: Pacific Geology, v. 8, p. 173–174.

Chappell, R., and Hine, R., 2006, The Cornubian Batholith: An example of magmatic fractionation on a crustal scale: Resource Geology, v. 56, p. 203–244, https://doi.org/10.1111/j.1751-3928.2006.tb00281.x.

Charles, J.-H., Whitehouse, M.J., Andersen, J.C.Ø., Shail, R.K., and Searle, M.P., 2018, Age and petrogenesis of the Lundy granite: Paleocene intraplate peraluminous magmatism in the Bristol Channel, UK: Journal of the Geological Society, v. 175, p. 44–59, https://doi.org/10.1144/jgs2017-023.

Charoy, B., 1986, The genesis of the Cornubian batholith (SW England): The example of the Carnmenellis pluton: Journal of Petrology, v. 27, p. 571–604, https://doi.org/10.1093/petrology/27.3.571.

Chen, Y., Clark, A.H., Farrar, E., Wasteneys, H., Hodgson, M.J., and Bromley, A.V., 1993, Diachronous and independent histories of plutonism and mineralisation in the Cornubian batholith, SW England: Journal of the Geological Society, v. 150, p. 1183–1191, https://doi.org/10.1144/gsjgs.150.6.1183.

Chesley, J.T., Halliday, A.N., Snee, L.W., Mezger, K., Shepherd, T., and Scrivener, R.C., 1993, Thermochronology of the Cornubian batholith in SW England: Implication for pluton emplacement and protracted hydrothermal mineralisation: Geochimica et Cosmochimica Acta,v. 57, p. 1817–1835, https://doi.org/10.1016/0016-7037(93)90115-D.

Clemens, J.D., 2003, S-type granite magmas: Petrogenetic issues, models and evidence: Earth-Science Reviews, v. 61, p. 1–18, https://doi.org/10.1016/S0012-8252(02)00107-1.

Clemens, J.D., 2012, Granite magmatism, from source to emplacement: A personal view: Applied Earth Science: Transactions of the Institution of Mining and Metallurgy, v. 121, p. 107–136.

Clemens, J.D., and Mawer, C.K., 1992, Granite magma transport by fracture propagation: Tectonophysics,v. 204, p. 339–360, https://doi.org/10.1016/0040-1951(92)90316-X.

Clemens, J.D., Stevens, G., and Farina, F., 2011, The enigmatic sources of I-type granites: The peritectic connection: Lithos, v. 126, p. 174–181, https://doi.org/10.1016/j.lithos.2011.07.004.

Clemens, J.D., Helps, P.A., Stevens, G., and Petford, N., 2021, Origins and scales of compositional variations in crustally: Derived granitic rocks: The example of the Dartmoor Pluton in the Cornubian batholith of Southwest Britain: The Journal of Geology, v. 129, p. 131– 169, https://doi.org/10.1086/714174.

Collins, W.J., Beams, S.D., White, A.J.R., and Chappell, B.W., 1982, Nature and origin of A-type granites withparticular reference to southeastern Australia: Contributions to Mineralogy and Petrology, v. 80, p. 189–200, https://doi.org/10.1007/BF00374895.

Cruden, A.R., 1998, On the emplacement of tabular granites: Journal of the Geological Society, v. 155, p. 853–862, https://doi.org/10.1144/gsjgs.155.5.0853.

Cruden, A.R., and Weinberg, R.F., 2018, Mechanism of magma transport and storage in the lower and middle crust: Magma segregation, ascent and emplacement, *in* Burchardt, S., ed., Volcanic and Igneous Plumbing Systems: Understanding Magma Transport, Storage, and Evolution in the Earth's Crust: Amsterdam, Elsevier, p. 13–53, https://doi.org/10.1016/B978-0-12-809749-6.00002-9.

Darbyshire, D., and Shepherd, T.J., 1985, Chronology of granite magmatism and associated mineralisation, SW England: Journal of the Geological Society, v. 142, p. 1159–1177, https://doi.org/10.1144/gsjgs.142.6.1159.

Darbyshire, D., and Shepherd, T.J., 1994, Nd and Sr isotope constraints on the origin of the Cornubian batholith, SW England: Journal of the Geological Society, v. 151, p. 795–802, https://doi.org/10.1144/gsjgs.151.5.0795. De La Beche, H.T., 1839, Report on the Geology of Cornwall, Devon and West Somerset: London, H.M. Stationery Office, 648 p.

Dijkstra, A.H., and Hatch, C., 2018, Mapping a hidden terrane boundary in the mantle lithosphere with lamprophyres: Nature Communications, v. 9, no. 3770, https://doi.org/10.1038/s41467-018-06253-7.

D'Lemos, R.S., Brown, M., and Strachan, R.A., 1992, Granite magma generation, ascent and emplacement within a transpressional orogen: Journal of the Geological Society, v. 149, p. 487–490, https://doi.org/10.1144/gsjgs.149.4.0487.

Duchoslav, M., Marks, M.A.W., Drost, K., McCammon, C.M., Marschall, H.R., Wenzel, T., and Markl, G., 2017, Changes in tourmaline composition during magmatic and hydrothermal processes leading to tin-ore deposition: The Cornubian Batholith, SW England: Ore Geology Reviews, v. 83, p. 215–234, https://doi.org/10.1016/j.oregeorev.2016.11.012.

Dupuis, N.E., Braid, J.A., Murphy, J.B., Shail, R.K., Archibald, D.A., and Nance, R.D., 2015, $^{40}Ar/^{39}Ar$ phlogopite geochronology of lamprophyre dykes in Cornwall, UK: New age constraints on Early Permian post-collisional magmatism in the Rhenohercynian Zone, SW England: Journal of the Geological Society, v. 172, p. 566–575, https://doi.org/10.1144/jgs2014-151.

Dupuis, N.E., Murphy, J.B., Braid, J.A., Shail, R.K., and Nance, R.D., 2016, Mantle evolution in the Variscides of SW England: Geochemical and isotopic constraints from mafic rocks: Tectonophysics, v. 681, https://doi.org/10.1016/j.tecto.2016.02.044.

Edmonds, E.A., Wright, J., Beer, K., Hawkes, J.R., Williams, M., Freshney, E., and Fenning, P.J., 1968, Geology of the Country around Okehampton: Memoir of the Geological Survey of Great Britain: London, H.M. Stationery Office.

Exley, C.S., 1958, Magmatic differentiation and alteration in the St Austell granite: Quarterly Journal of the Geological Society, v. 114, p. 197–230, https://doi.org/10.1144/gsjgs.114.1.0197.

Exley, C.S., 1996, Petrological features of the Bodmin Moor Granite, Cornwall: Proceedings of the Ussher Society,v. 9, p. 85–90.

Exley, C.S., and Stone, M., 1982, Hercynian intrusive rocks, *in* Sutherland, D.S., ed., Igneous Rocks of the British Isles: Chichester, UK, Wiley, p. 287–320.

Exley, C.S., Stone, M., and Floyd, P., 1983, Composition and Petrogenesis of the Cornubian Granite Batholith and post-orogenic volcanic rocks in Southwest England, *in* Hancock, P.L., ed., The Variscan Fold Belt of the British Isles: Bristol, UK, Adam Hilger, p. 153–177.

Farndale, H., and Law, R., 2022, An update on the United Downs Geothermal Power Project, Cornwall, UK: Proceedings of Fourth Workshop on Geothermal Reservoir Engineering, Stanford University, California, USA, p. 1–13.

Floyd, P.A., Exley, C.S., and Styles, M.T., 1993, The Igneous Rocks of South-West England: Dordrecht, Netherlands, Springer Science and Business Media, https://doi.org/10.1007/978-94-011-1502-5.

Franke, W., 2024, The Rheic riddle: Ocean closed, but no orogen, *in* Nance, R.D., Strachan, R.A., Quesada, C., and Lin, S., Supercontinents, Orogenesis and Magmatism: Geological Society, London, Special Publications 542, https://doi.org/10.1144/SP542-2022-354.

Glazner, A.F., and Bartley, J.M., 2006, Is stoping a volumetrically significant emplacement process?: Geological Society of America Bulletin, v. 120, p. 1082–1087, https://doi.org/10.1130/B25738.1.

Hall, A., 1971, Greisenisation in the Granite of Cligga Head, Cornwall: Proceedings of the Geologists' Association, v. 82, no. 2, p. 209–230, https://doi.org/10.1016/S0016-7878(71)80003-2.

Hill, P.L., and Manning, D., 1987, Multiple intrusions and pervasive hydrothermal alteration in the St Austell granite, Cornwall: Proceedings of the Ussher Society, v. 6, p. 447–453.

Hughes, S.P., Stickland, R.J., Shail, R.K., LeBoutillier, N.G., Alexander, A., and Thomas, M., 2009, The chronology and kinematics of Late Palaeozoic deformation in the NW contact metamorphic aureole of the Land's End Granite: Geoscience in South-west England, v. 12, p. 140–152.

Hutton, D., and Reavy, R.J., 1992, Strike-slip tectonics and granite petrogenesis: Tectonics, v. 11, no. 5, p. 960–967, https://doi.org/10.1029/92TC00336.

Ishihara, S., 1977, The magnetite-series and ilmenite-series Granitic rocks: Minería y Geología, v. 27, p. 293–305. Jackson, N.J., Willis-Richards, J., Manning, D.A.C., and Sams, M., 1989, Evolution of the Cornubian ore field, Southwest England: Part II, Mineral deposits and ore-forming processes: Economic Geology, v. 84, p. 1101–1133, https://doi.org/10.2113/gsecongeo.84.5.1101.

Jacob, J.-B., Moyen, J.-F., Fiannacca, P., Laurent, O., Bachmann, O., Janousek, V., Farina, F., and Villaros, A., 2021, Crustal melting vs. fractionation of basaltic magmas: Part 2, Attempting to quantify mantle and crustal contributions in granitoids: Lithos, v. 402-403, https://doi.org/10.1016/j.lithos.2021.106292.

Janousek, V., and Zák, J., 2015, Eurogranites 2015: A Field Guide to Variscan Plutons of the Bohemian massif: Czech Geological Survey, 167 p.

Jones, D.G., Miller, J.M., and Roberts, P.D., 1988, A seabed radiometric survey of Haig Fras, S Celtic Sea, UK: Proceedings of the Geologists' Association, v. 99, no. 3, p. 193–203, https://doi.org/10.1016/S0016-7878(88)80035-X.

Jones, R.H., 1991, A seismic reflection survey as part of a geophysical investigation of the Carnmenellis granite: Proceedings of the Ussher Society, v. 7, p. 418–420.

Kratinová, Z., Jevzek, J., Schulmann, K., Hrouda, F., Shail, R., and Lexa, O., 2010, Noncoaxial K-feldspar and AMS subfabrics in the Land's End granite, Cornwall: Evidence of magmatic fabric decoupling during late deformation and matrix crystallization: Journal of Geophysical Research: Solid Earth, v. 115, no. B9, https://doi.org/10.1029/2009JB006714.

Le Gall, B., 1990, Evidence of an imbricate crustal thrust belt in the southern Britain Variscides: Contribution of southwestern approaches traverse (SWAT) deep seismic reflection profiling recorded through the English Channel and the Celtic Sea: Tectonics, v. 9, p. 283–302, https://doi.org/10.1029/TC009i002p00283.

Leveridge, B.E., and Hartley, A.J., 2006, The Variscan Orogeny: The development and deformation of Devonian/ Carboniferous basins in SW England and South Wales, *in* Brenchley, P.J., and Rawson, P.F., eds., The Geology of England and Wales (second edition): Geological Society, London, Geology of Series, p. 225–255, https://doi.org/10.1144/GOEWP.10.

Leveridge, B.E., Holder, M.T., Goode, A., Scrivener, R.C., Jones, N.S., and Merriman, R.J., 2002, Geology of the Plymouth and south-east Cornwall area: Memoir of the British Geological Survey, sheet 348 (England and Wales).

Mackay-Champion, T., Searle, M.P., Tapster, S., Roberts, N., Shail, R.K., Palin, R.M., Willment, G., and Evans, J.T., 2024, Magmatic, metamorphic and structural history of the Variscan Lizard Ophiolite, Cornwall, UK and its metamorphic sole: Tectonics (in press).

Manning, D.A.C., and Exley, C.S., 1984, The origins of latestage rocks in the St Austell granite: A re-interpretation: Journal of the Geological Society, v. 141, p. 581–591, https://doi.org/10.1144/gsjgs.141.3.0581.

Manning, D.A.C., Hill, P., and Howe, J., 1996, Primary lithological variation in the kaolinised St Austell granite, Cornwall, England: Journal of the Geological Society, v. 153, p. 827–838, https://doi.org/10.1144/gsjgs.153.6.0827.

Michel, J., Baumgartner, L., Putlitz, B., Schaltegger, U., and Ovtcharova, M., 2008, Incremental growth of the Patagonian Torres del Paine laccolith over 90 k.y.: Geology, v. 36, p. 459–462, https://doi.org/10.1130/G24546A.1.

Moore, J.M., and Jackson, N., 1977, Structure and mineralisation in the Cligga granite stock, Cornwall: Journal of the Geological Society, v. 133, p. 467–480, https://doi .org/10.1144/gsjgs.133.5.0467.

Müller, A., Seltmann, R., Halls, C., Siebel, W., Dulski, P., Jeffries, T., Spratt, J., and Kronz, A., 2006, The magmatic evolution of the Land's End pluton, Cornwall, and associated pre-enrichment of metals: Ore Geology Reviews, v. 28, no. 3, p. 329–367, https://doi.org/10.1016/j.oregeorev.2005.05.002.

Nance, R.D., Neace, E.R., Braid, J.A., Murphy, J.B., Dupuis, N., and Shail, R.K., 2015, Does the Meguma terrane extend into SW England?: Geoscience Canada, v. 42, p. 61–76, https://doi.org/10.12789/geocanj.2014.41.056.

Neace, E.R., Nance, D., Murphy, B., Lancaster, P.J., and Shail, R.K., 2016, Zircon LA-ICPMS geochronology of the Cornubian batholith, SW England: Tectonophysics, v. 681, p. 332–352, https://doi.org/10.1016/j.tecto.2016.04.002.

Ng, S.W.-P., Chung, S.-L., Robb, L.J., Searle, M.P., Ghani, A.A., Whitehouse, M.J., Oliver, G.J.H., Sone, M., Gardiner, N.J., and Roselee, M.H., 2015, Petrogenesis of Malaysian granitoids in the Southeast Asia tin belt: Part 1. Geochemical and Sr-Nd isotopic characteristics: Geological Society of America Bulletin, v. 127, p. 1209–1237, https://doi.org/10.1130/B31213.1.

Petford, N., Kerr, R.C., and Lister, J.R., 1993, Dike transport of granitoid magmas: Geology, v. 21, p. 845–848, https:// doi.org/10.1130/0091-7613(1993)021<0845:DTOGM>2.3.CO;2.

Pitcher, W., 1979, The nature, ascent and emplacement of granitic magmas: Journal of the Geological Society, v. 136, p. 627–662, https://doi.org/10.1144/gsjgs.136.6.0627.

Pownall, J.M., Waters, D.J., Searle, M.P., Shail, R.K., and Robb, L.J., 2012, Shallow laccolith emplacement of the Land's End and Tregonning granites: Cornwall, UK: Evidence from aureole field relations and P-T modelling of cordierite-anthophyllite hornfels: Geosphere, v. 8, p. 1467–1504, https://doi.org/10.1130/GES00802.1.

Rattey, P.R., and Sanderson, D.J., 1984, The structure of SW Cornwall and its bearing on the emplacement of the Lizard complex: Journal of the Geological Society, v. 141, p. 87–95, https://doi.org/10.1144/gsjgs.141.1.0087.

Read, H.H., 1948, Granites and granites, *in* Gilluly, J., ed., Origin of Granite: Geological Society of America Memoir 28, p. 1–20, https://doi.org/10.1130/MEM28-p1.

Reichardt, H., and Weinberg, R.F., 2012, The dike swarm of the Karakoram shear zone, Ladakh, NW India: Linking granite source to batholith: Geological Society of America Bulletin, v. 124, p. 89–103, https://doi.org/10.1130/B30394.1.

Reinecker, J., Gutmanis, J., Foxford, A., Cotton, L., Dalby, C., and Law, R., 2021, Geothermal exploration and reservoir modelling of the United Downs deep geothermal project, Cornwall (UK): Geothermics, v. 97, https://doi.org/10.1016/j.geothermics.2021.102226.

Romer, R.L., and Kroner, U., 2016, Phanerozoic tin and tungsten mineralisation-tectonic controls on the distribution of enriched protoliths and heat sources for crustal melting: Gondwana Research, v. 31, p. 60–95, https://doi.org/10.1016/j.gr.2015.11.002.

Sams, M.S., and Thomas-Betts, A., 1988, Models of convective fluid flow and mineralization in southwest England: Journal of the Geological Society, v. 145, p. 809–817, https://doi.org/10.1144/gsjgs.145.5.0809.

Sawyer, E.W., Cesare, B., and Brown, M., 2011, When the continental crust melts: Elements, v. 7, no. 4, p. 229– 234, https://doi.org/10.2113/gselements.7.4.229.

Scaillet, B., Pichavant, M., and Roux, J., 1995, Experimental crystallization of leucogranite magmas: Journal of Petrology, v. 36, p. 663–705, https://doi.org/10.1093/petrology/36.3.663.

Scrivener, J.B., 1903, The Granite and Greisen of Cligga Head (Western Cornwall): Quarterly Journal of the Geological Society, v. 59, p. 142–159,

https://doi.org/10.1144/GSL.JGS.1903.059.01-04.16.

Scrivener, R.C., Darbyshire, D.P.F., and Shepherd, T.J., 1994, Timing and significance of cross-course mineralization in SW England: Journal of the Geological Society,v. 151, p. 587–590, https://doi.org/10.1144/gsjgs.151.4.0587.

Searle, M., 2013, Crustal melting, ductile flow, and deformation in mountain belts: Cause and effect relationships: Lithosphere, v. 5, p. 547–554, https://doi.org/10.1130/RF.L006.1.

Searle, M.P., 1999, Emplacement of Himalayan leucogranites by magma injection along giant sill complexes: Examples from the Cho Oyu, Gyachung Kang, and Everest leucogranites (Nepal Himalaya): Journal of Asian Earth Sciences, v. 17, p. 773–783, https://doi.org/10.1016/S1367-9120(99)00020-6.

Searle, M.P., 2015, Mountain Building, Tectonic Evolution, Rheology, and Crustal Flow in the Himalaya, Karakoram, and Tibet, *in* Schubert, G., ed., Treatise on Geophysics (second edition), Volume 6: Crustal and Lithosphere Dynamics: Amsterdam, Elsevier, p. 469– 511, https://doi.org/10.1016/B978-0-444-53802-4.00121-4.

Searle, M.P., Parrish, R.R., Hodges, K.V., Hurford, A., Ayres, M.W., and Whitehouse, M.J., 1997, Shisha Pangma Leucogranites, South Tibetan Himalaya: Field relations, geochemistry, age, origin and emplacement: The Journal of Geology, v. 105, p. 295–318, https://doi.org/10.1086/515924.

Searle, M.P., Simpson, R.L., Law, R.D., Parrish, R.R., and Waters, D.J., 2003, The structural geometry, metamorphic and magmatic evolution of the Everest massif, High Himalaya of Nepal-South Tibet: Journal of the Geological Society, v. 160, p. 345–366, https://doi.org/10.1144/0016-764902-126.

Searle, M.P., Cottle, J.M., Streule, M.J., and Waters, D.J., 2009, Crustal melt granites and migmatites along the Himalaya: Melt source, segregation, transport and granite emplacement mechanisms: Transactions of the Royal Society of Edinburgh: Earth Sciences, v. 100, p. 219–233, https://doi.org/10.1017/S175569100901617X.

Searle, M.P., Parrish, R.R., Thow, A.V., Noble, S.R., Phillips, R.J., and Waters, D.J., 2010, Anatomy, age and evolution of a collisional mountain belt: The Baltoro batholith and Karakoram Metamorphic complex, Pakistan: Journal of the Geological Society, v. 167, p. 183–202, https://doi.org/10.1144/0016-76492009-043.

Searle, M.P., Roberts, N.M.W., Chung, S.-L., Lee, Y.-H., Cook, K.L., Elliott, J.R., Weller, O., St-Onge, M.R., Xu, X.-W., Tan, X.B., and Li, K., 2016, Age and anatomy of the Gongga Shan batholith, eastern Tibet plateau and its relationship to active Xianshui-he fault: Geosphere, v. 12, no. 3, p. 948–970, https://doi.org/10.1130/GES01244.1.

Shail, R.K., and Alexander, A.C., 1997, Late Carboniferous to Triassic reactivation of Variscan basement in the western English Channel: Evidence from onshore exposures in south Cornwall: Journal of the Geological Society, v. 154, p. 163–168, https://doi.org/10.1144/gsjgs.154.1.0163.

Shail, R.K., and Leveridge, B.E., 2009, The Rhenohercynian passive margin of SW England: Development, inversion and extensional reactivation: Comptes Rendus Geoscience, v. 341, p. 140–155, https://doi.org/10.1016/j.crte.2008.11.002.

Shail, R.K., and Wilkinson, J.J., 1994, Lateto post-Variscan extensional tectonics in south Cornwall: Proceedings of the Ussher Society, v. 8, p. 262–270.

Shail, R.K., Stuart, F.M., Wilkinson, J.J., and Boyce, A.J., 2003, The role of post-Variscan extensional tectonics and mantle melting in the generation of the Lower Permian granites and the giant W-As-Sn-Cu-Zn-Pb orefield of SW England: Transactions of the Institutions of Mining and Metallurgy, http://hdl.handle.net/10036/3644.

Shail, R.K., Andersen, J., Simons, B., and Williamson, B., 2014, Eurogranites 2014: Granites and Mineralisation of SW England: Field Excursion Guidebook: Penryn, UK, Camborne School of Mines, University of Exeter, 147 p.

Sillitoe, R.H., and Lehmann, B., 2022, Copper-rich tin deposits: Mineralium Deposita, v. 57, no. 1, p. 1–11, https://doi.org/10.1007/s00126-021-01078-9.

Simons, B., Shail, R.K., and Andersen, J.Ø., 2016, The petrogenesis of the Early Permian Variscan granites of the Cornubian Batholith: Lower plate post-collisional peraluminous magmatism in the Rhenohercynian zone of SW England: Lithos, v. 260, p. 76–94, https://doi.org/10.1016/j.lithos.2016.05.010.

Simons, B., Andersen, J.Ø., Shail, R.K., and Jenner, F.E., 2017, Fractionation of Li, Be, Ga, Nb, Ta, In, Sn, Sb, W, and Bi in the peraluminous Early Permian Variscan granites of the Cornubian batholith: Precursor processes to magmatic-hydrothermal mineralisation: Lithos, v. 278–281, p. 491–512, https://doi.org/10.1016/j.lithos.2017.02.007.

Smith, W.D., Darling, J.R., Bullen, D.S., Lasalle, S., Pereira, I., Moreira, H., Allen, C.J., and Tapster, S., 2019, Zircon perspectives on the age and origin of evolved Stype granites from the Cornubian batholith, Southwest Britain: Lithos, v. 336–337, p. 14–26, https://doi.org/10.1016/j.lithos.2019.03.025.

Stimac, J.A., Clark, A.H., Chen, Y., and Garcia, S., 1995, Enclaves and their bearing on the origin of the Cornubian batholith, SW England: Mineralogical Magazine, v. 59, p. 273–296, https://doi.org/10.1180/minmag.1995.059.395.12.

Stone, M., 1971, Form and structure of the granites of SouthWest England: Symposium on Structure of South-West England: Proceedings of the Ussher Society, v. 2, p. 253–263.

Stone, M., 1975, Structure and petrology of the TregonningGodolphin granite, Cornwall: Proceedings of the Geologists' Association, v. 86, no. 2, p. 155–170, https://doi.org/10.1016/S0016-7878(75)80098-8.

Stone, M., 1992, The Tregonning granite: Petrogenesis of Limica granites in the Cornubian batholith: Mineralogical Magazine, v. 56, p. 141–155, https://doi.org/10.1180/minmag.1992.056.383.01.

Stone, M., 1995, The main Dartmoor granites: Petrogenesis and comparisons with the Carnmenellis and Isles of Scilly granites: Proceedings of the Ussher Society, v. 8, p. 379–384.

Stone, M., 2000, The Early Cornubian plutons: A geochemistry study, comparisons and some implications: Proceedings of the Usher Society, v. 10, p. 37–41.

Stone, M., and Exley, C.S., 1984, Emplacement of the Porthmeor granite pluton, west Cornwall:

Proceedings of the Ussher Society, v. 6, p. 42–45.

Stone, M., and Exley, C.S., 1985, High heat production granites of southwest England and their associated mineralization: A review: Institution of Mining and Metallurgy Conference on high heat production (HHP) granites, hydrothermal circulation and ore genesis, p. 571–593. Tapster, S., and Bright, J.W.G., 2020, High-precision IDTIMS cassiterite U-Pb systematics using a low-contamination hydrothermal decomposition: Implications for LA-ICP-MS and ore deposit geochronology: Geochronology, v. 2, p. 425–441, https://doi.org/10.5194/gchron-2-425-2020.

Taylor, G.K., 2007, Pluton shape in the Cornubian Batholith: New perspectives from gravity modelling: Journal of the Geological Society, v. 164, p. 525–528, https://doi.org/10.1144/0016-76492006-104.

Tilley, C.E., 1935, Metasomatism associated with the greenstone-hornfelses of Kenidjack and Botallack: Mineralogical Magazine, v. 24, p. 181–202, https://doi.org/10.1180/minmag.1935.024.151.01.

Ussher, W.A.E., 1892, The British Culm Measures: Proceedings of the Somerset Archaeological and Natural History Society, v. 38, p. 111–219.

Watts, A.B., Xu, C., Searle, M.P., Jurkowski, C., and Shail, R.K., 2024, Permian Cornubian granite batholith of SW England; Part 2: Gravity anomalies, structure and state of isostasy: Geological Society of America Bulletin (in press), https://doi.org/10.1130/B37459.1.

Weinberg, R.F., and Mark, G., 2008, Magma migration, folding and disaggregation of migmatites in the Karakoram shear zone, Ladakh, NW India: Geological Society of America Bulletin, v. 120, p. 994–1009, https://doi.org/10.1130/B26227.1.

Weinberg, R.F., and Podladkicov, Y., 1994, Diapiric ascent of magmas through power law crust and mantle: Journal of Geophysical Research: Solid Earth, v. 99, B5, p. 9543–9559, https://doi.org/10.1029/93JB03461. Weinberg, R.F., and Searle, M.P., 1998, The Pangong Injection complex, Indian Karakoram: A case of pervasive granite flow through a hot, viscous crust: Journal of the Geological Society, v. 155, p. 883–891, https://doi.org/10.1144/gsjgs.155.5.0883.

Weinberg, R.F., and Searle, M.P., 1999, Volatile-assisted intrusion and autometasomatism of leucogranites in the Khumbu Himalaya, Nepal: The Journal of Geology, v. 107, p. 27–48, https://doi.org/10.1086/314330. Whalen, J.B., Currie, K.L., and Chappell, B.W., 1987, A-type granites: Geochemical characteristics, discrimination and petrogenesis: Contributions to Mineralogy and Petrology, v. 95, p. 407–419, https://doi.org/10.1007/BF00402202.

White, A.J.R., and Chappell, B.W., 1977, Ultrametamorphism and granite genesis: Tectonophysics, v. 43, p. 7– 22, https://doi.org/10.1016/0040-1951(77)90003-8.

Williamson, B., Müller, A., and Shail, R.K., 2010, Source and partitioning of B and Sn in the Cornubian batholith of southwest England: Ore Geology Reviews, v. 38, no. 1–2, p. 1–8, https://doi.org/10.1016/j.oregeorev.2010.05.002.

Williamson, B.J., Spratt, J., Adams, J.T., Tindle, A.G., and Stanley, C.J., 2000, Geochemical constraints from zoned hydrothermal tourmalines on fluid inclusion and Sn mineralisation:

An example from fault breccias at Roche, SW England: Journal of Petrology, v. 41, p. 1439–1453, https://doi.org/10.1093/petrology/41.9.1439.

Willis-Richards, J., and Jackson, N.J., 1989, Evolution of the Cornubian ore field, Southwest England: Part I, Batholith modeling and ore distribution: Economic Geology, v. 84, p. 1078–1100, https://doi.org/10.2113/gsecongeo.84.5.1078.

Woodcock, N.H., Soper, N.J., and Strachan, R.A., 2007, A Rheic cause for the Acadian deformation in Europe: Journal of the Geological Society, v. 164, no. 5, p. 1023–1036, https://doi.org/10.1144/0016-76492006-129.

Ziegler, P.A., and Dèzes, P., 2006, Crustal evolution of Western and Central Europe, *in* Gee, D.G., and Stephenson, R.A., eds., European Lithosphere Dynamics: Geological Society, London, Memoir 32, p. 43–56, https://doi.org/10.1144/GSL.MEM.2006.032.01.03.

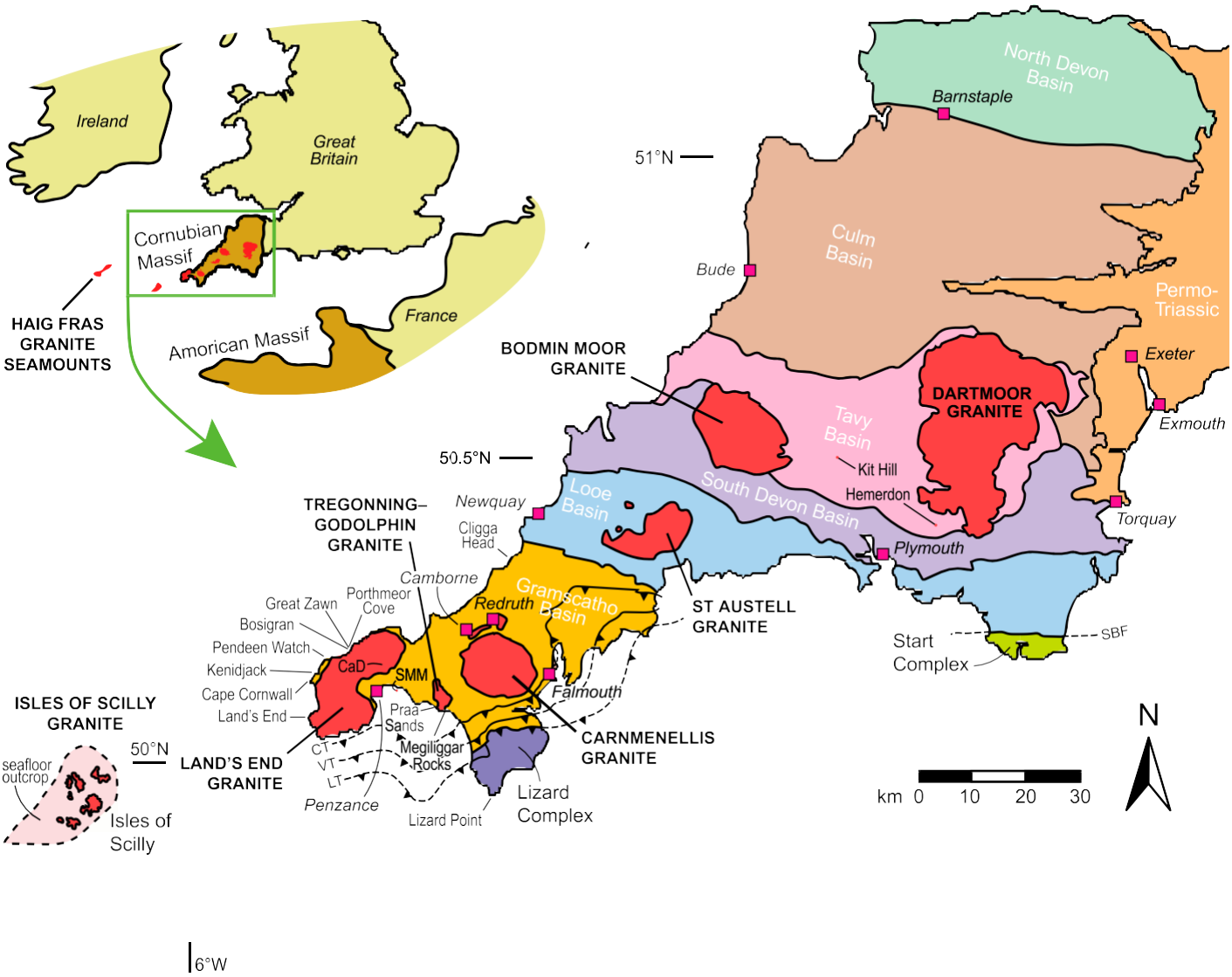

Figure 1. Geological map of SW England showing the major granite plutons and major structures, after Exley and Stone (1982) and Floyd et al. (1993), and sedimentary basins, after Shail and Leveridge (2009). The submarine extent of the Isles of Scilly granite is from the British Geological Survey (1982). Inset map, top left, shows the location of the Cornubian Massif in the southern British Isles and the region of interest in the green box. Faults labeled are: CT—Carrick thrust; VT—Veryan thrust; LT—Lizard thrust; SBF—Start boundary fault. SMM—St Michael's Mount; CaD—Castle-an-Dinas.

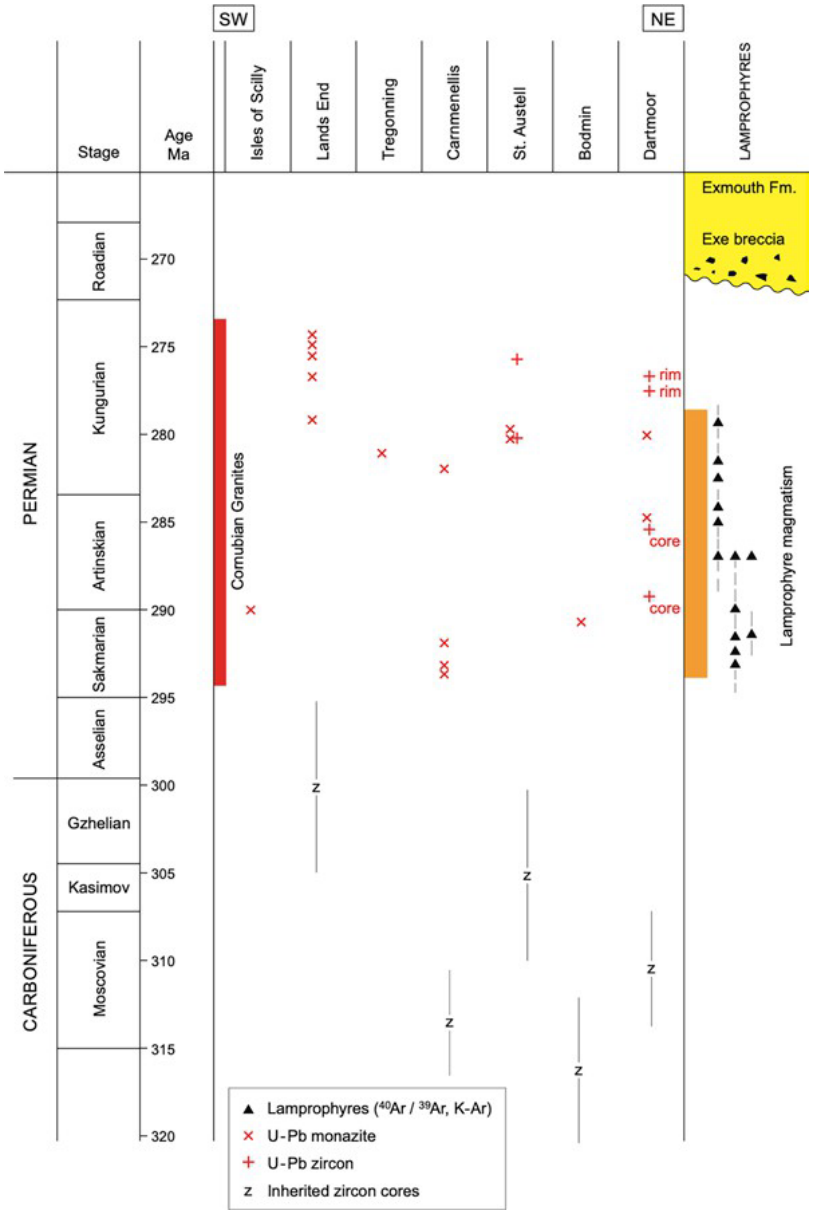

Figure 2. U-Pb ages of individual plutons along the Cornubian batholith of SW England, after Chen et al. (1993), Chesley et al. (1993), and Smith et al. (2019). Zircon laser ablation–inductively coupled plasma–mass spectrometry ages from Neace et al. (2016) are all consistently older than the monazite ages and thought to have some inherited component. K-Ar and 40Ar-39Ar ages of lamprophyre dikes are from Dupuis et al. (2015). Fm.—Formation.

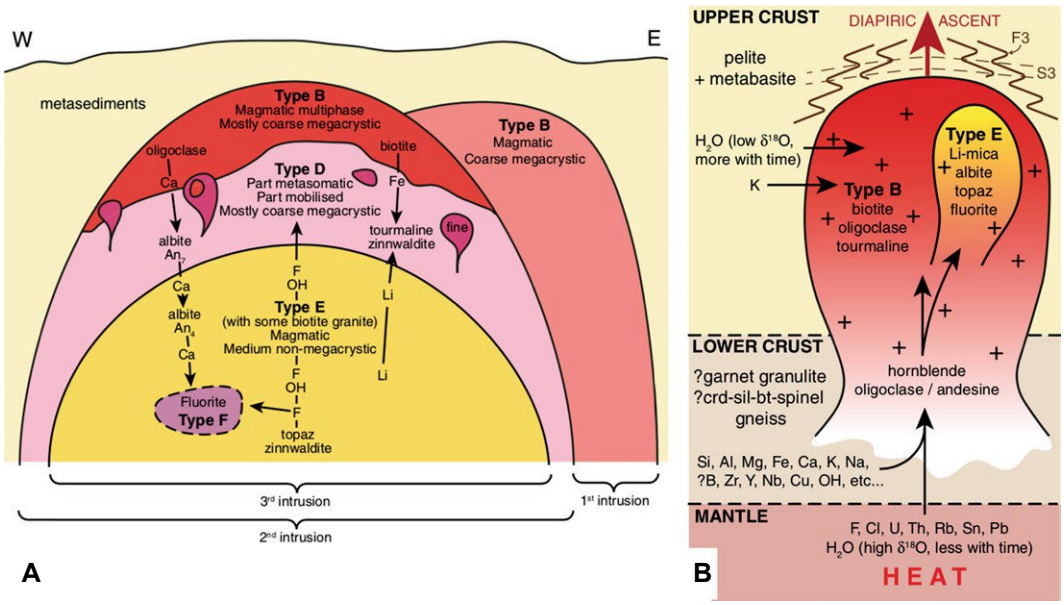

Figure 3. (A) The St Austell model for SW England granites and (B) the 1980s model, after Floyd et al. (1993). See text for discussion. An—anorthite; bt—biotite; crd—cordierite; sil—sillimanite.

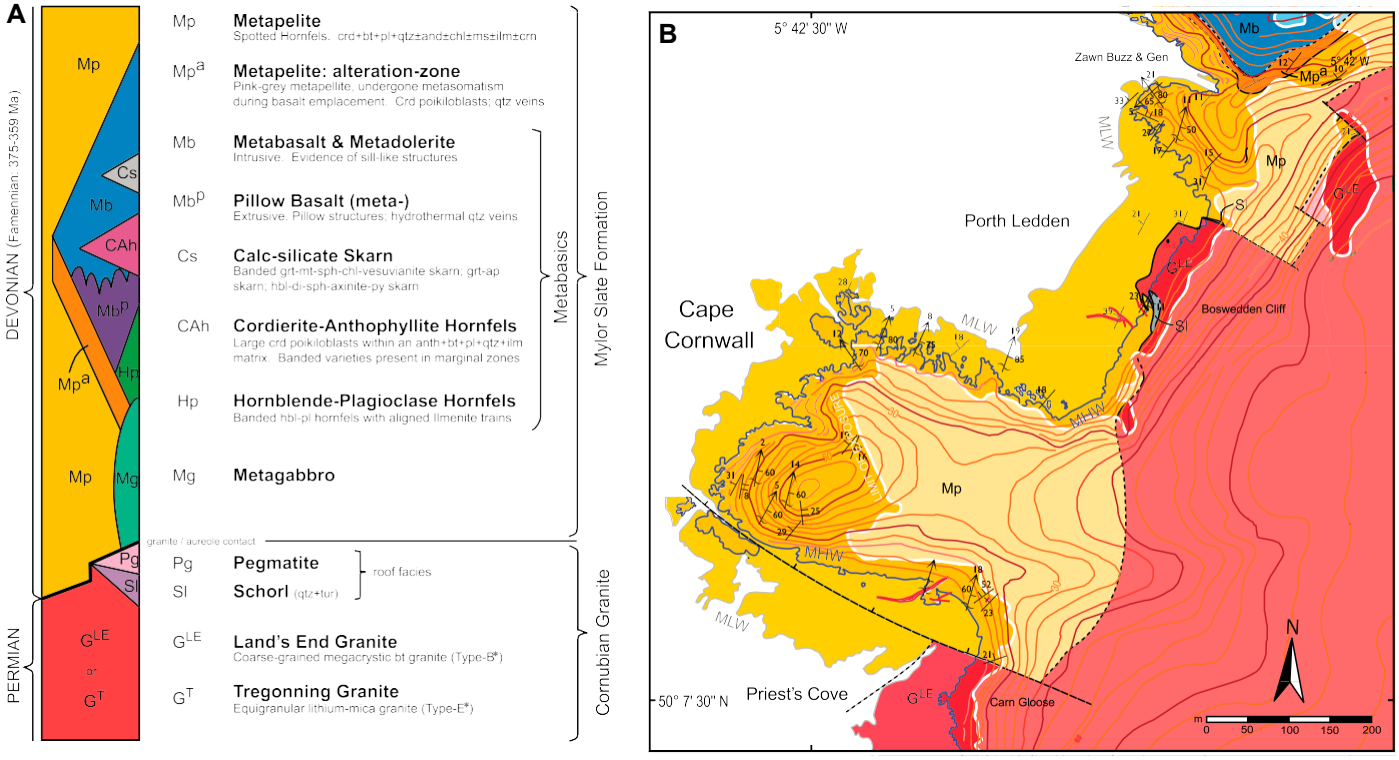

Figure 4. (A) Stratigraphic components of the Land's End granite of SW England and its contact metamorphic aureole, after Pownall et al. (2012). Granite classification from Exley et al. (1983). (B) Geological map of the Cape Cornwall area, northern part of the Land's End granite, showing granite contact localities at Priest's cove and Porth Ledden, after Pownall et al. (2012). MHW and MLW indicate the mean high and low water marks, respectively. The intertidal zone is shaded in a paler color. and—andalusite; anth—anthophyllite; ap—apatite; bt—biotite; chl—chlorite; crd—cordierite; crn—corundum; di—diopside; grt—garnet; hbl—hornblende; ilm—ilmenite; ms—muscovite; mt—magnetite; pl—plagioclase; py—pyrite; qtz—quartz; sil—sillimanite; sph—sphene; tur—tourmaline.

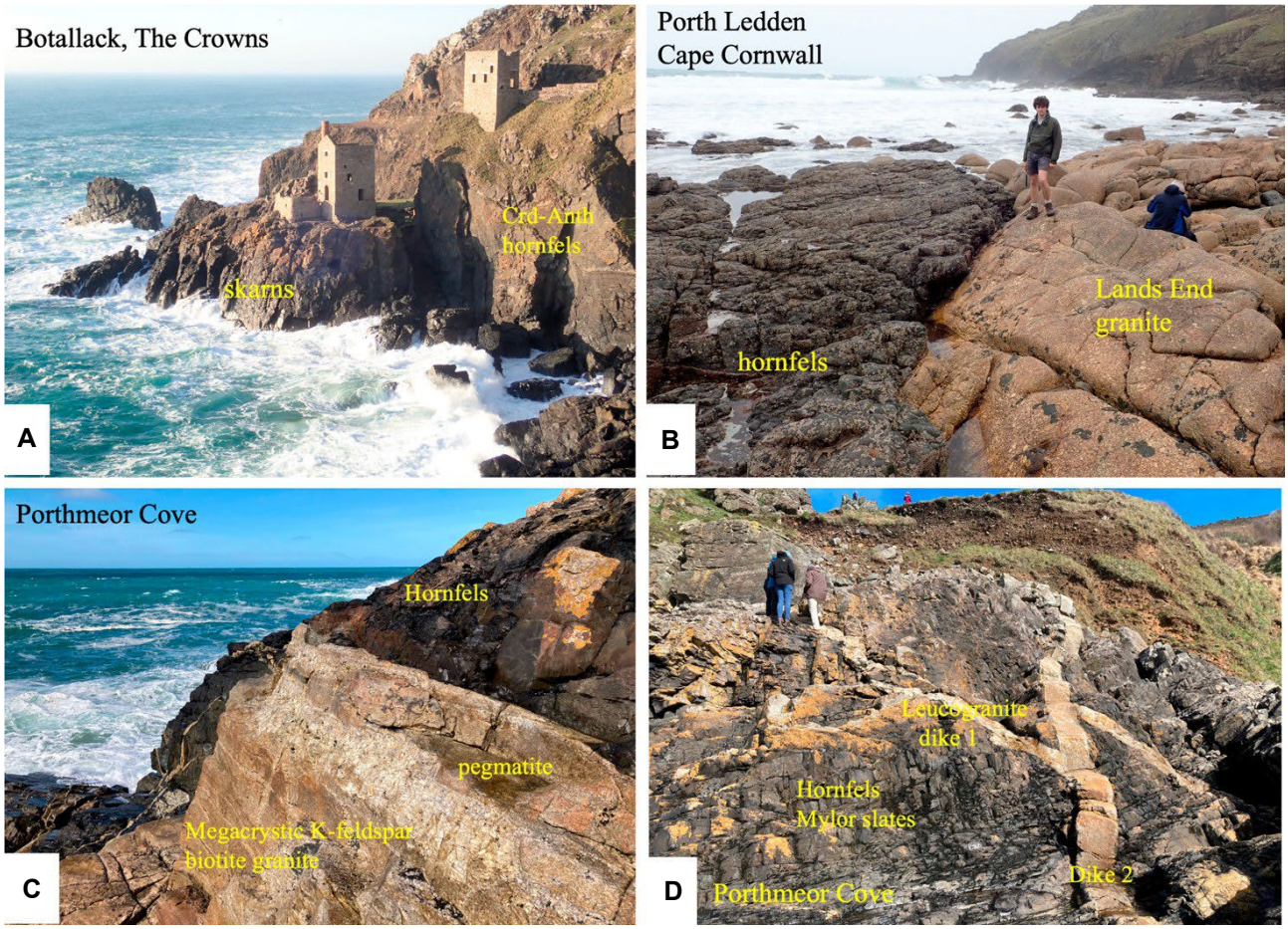

Figure 5. (A) Engine houses at the Crowns, Botallack, mine of SW England built on skarns and hornfels around the margin of the Land's End granite. (B) Outward dipping granite contact at Porth Ledden, Cape Cornwall, showing hornfels in the Mylor Slate Formation country rock. (C) Roof complex of the southern cupola, Porthmeor Cove. Note pegmatites concentrated along the upper margin of the granite. (D) Two sets of leucogranite dikes emanating from the roof of the granite, Porthmeor Cove. Note the 1.5 m offset of set 1 dike by intrusion of the later set 2 leucogranite. Crd-Anth—cordierite–anthophyllite.

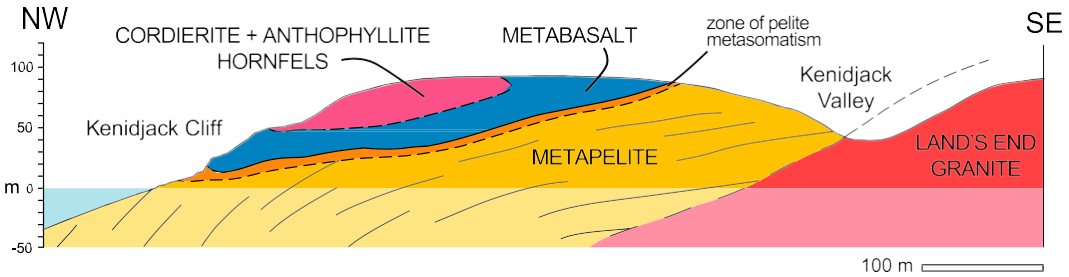

Figure 6. Sketch section across the upper margin of the Land's End granite at Kenidjack of SW England, showing the outwarddipping pluton contact, and metapelitic cordierite + andalusite hornfels, and meta-igneous cordierite + anthophyllite hornfels in the contact metamorphic aureole, modified after Pownall et al. (2012).

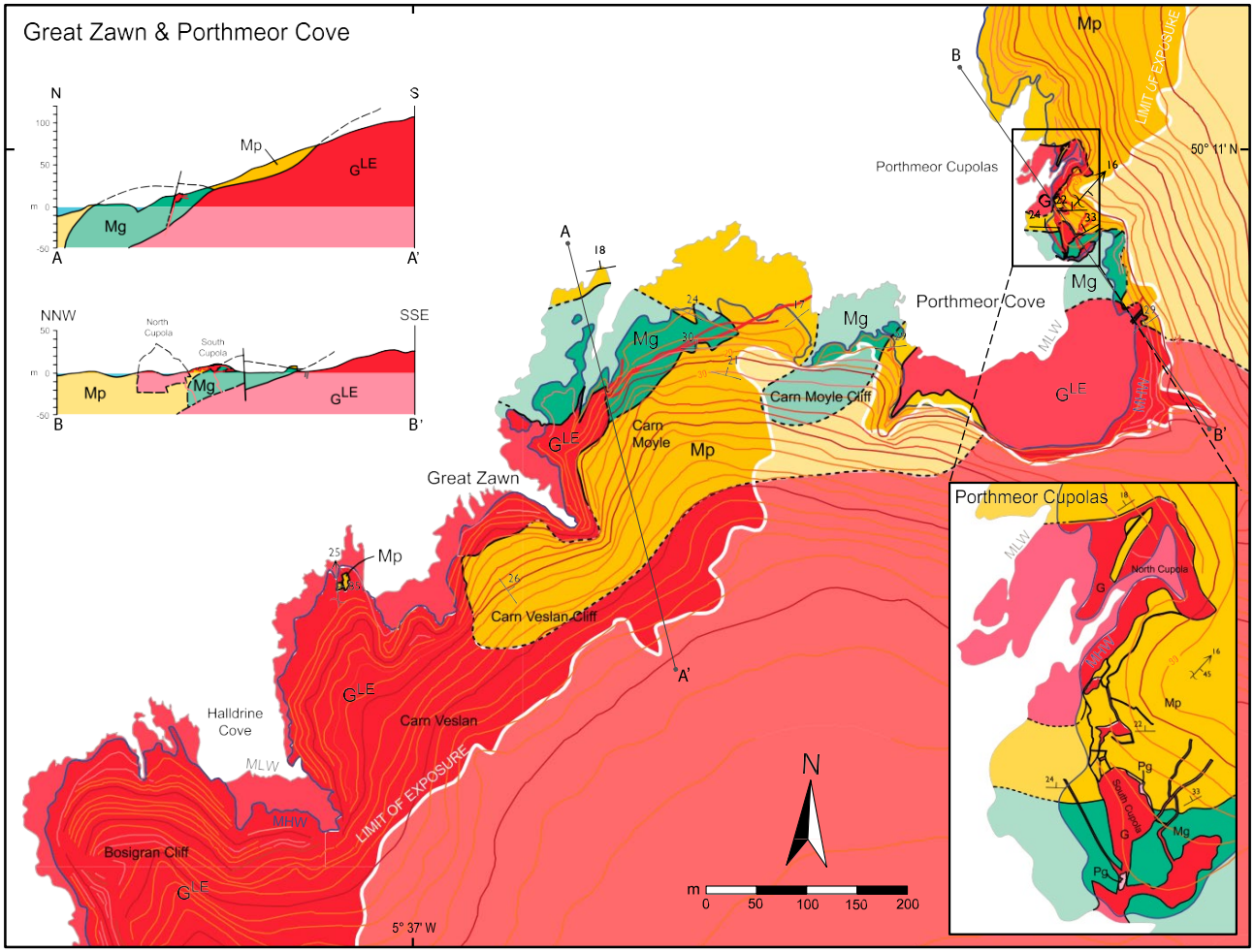

Figure 7. Geological map of the Great Zawn–Porthmeor Cove section along the northern margin of the Land's End granite of SW England, after Pownall et al. (2012). The positions of cross sections A–A′ and B–B′ (top left) are indicated on the main map. See Figure 4A for key to lithologies. MHW and MLW indicate the mean high and low water marks, respectively. The intertidal zone is shaded in a paler color.

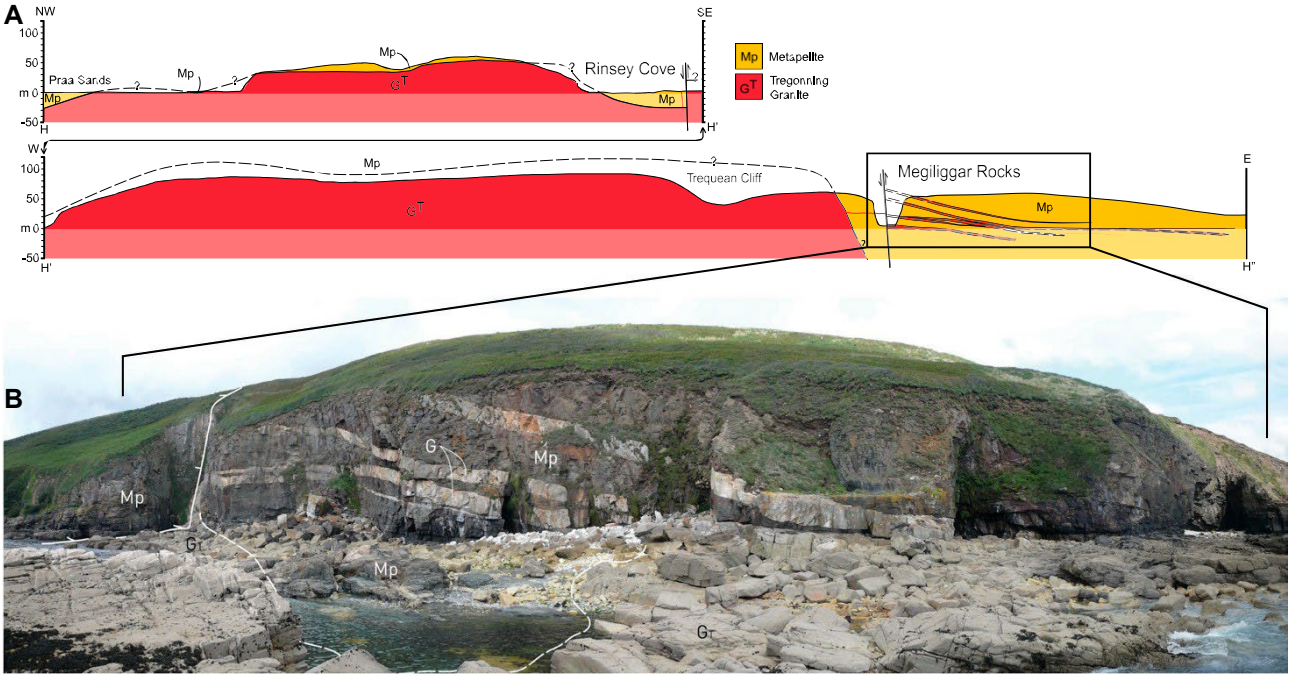

Figure 8. (A) West-east profile across the Tregonning granite, from Praa Sands, Rinsey Cove, and Megiliggar rocks of SW England. (B) The three horizontal leucogranites and aplite-pegmatite sills intruding into the contact metamorphosed Mylor Slate Formation, along the eastern margin of the Tregonning lithium mica, topaz granite. See Figure 4A for key to lithologies.

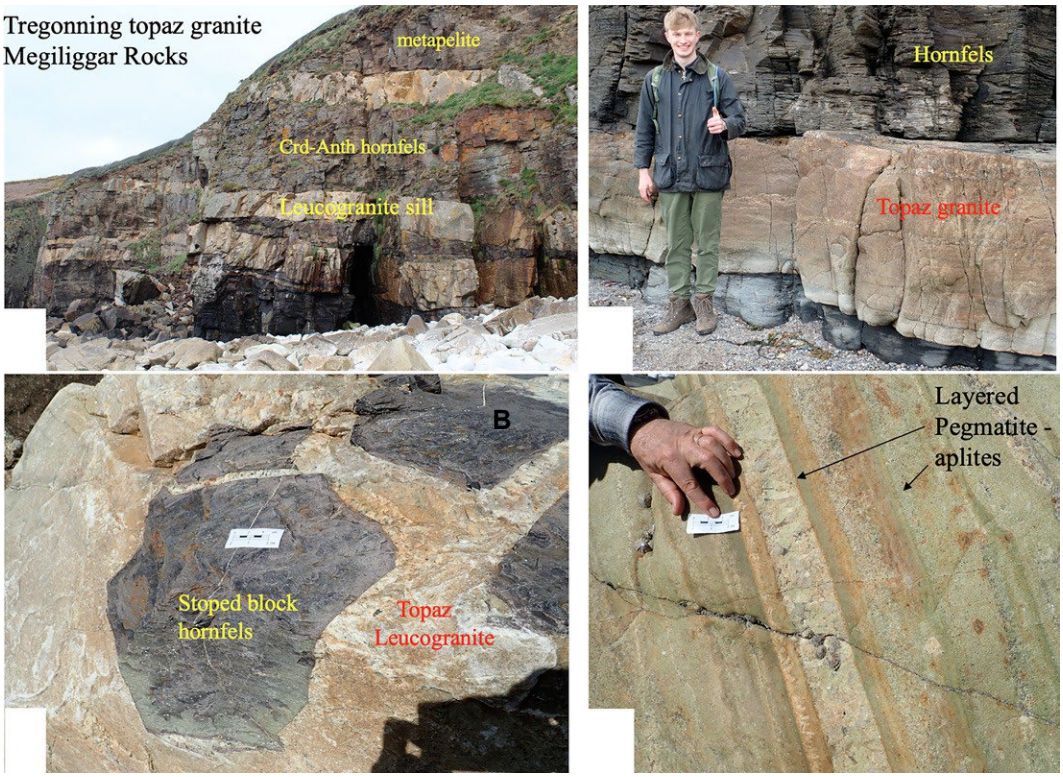

Figure 9. (A) Tregonning topaz granite sills intruding into the spotted hornfels of the contact metamorphic aureole, Megiliggar Rocks of SW England. (B) Banded aplite-pegmatite sill of topaz granite with sharp contact, intruding andalusite and cordierite hornfels. (C) Stoped block or xenolith of cordierite hornfels within the Tregonning topaz granite. (D) Banded pegmatite-aplite along the roof complex of the Tregonning granite. Crd-Anth—cordierite–anthophyllite.

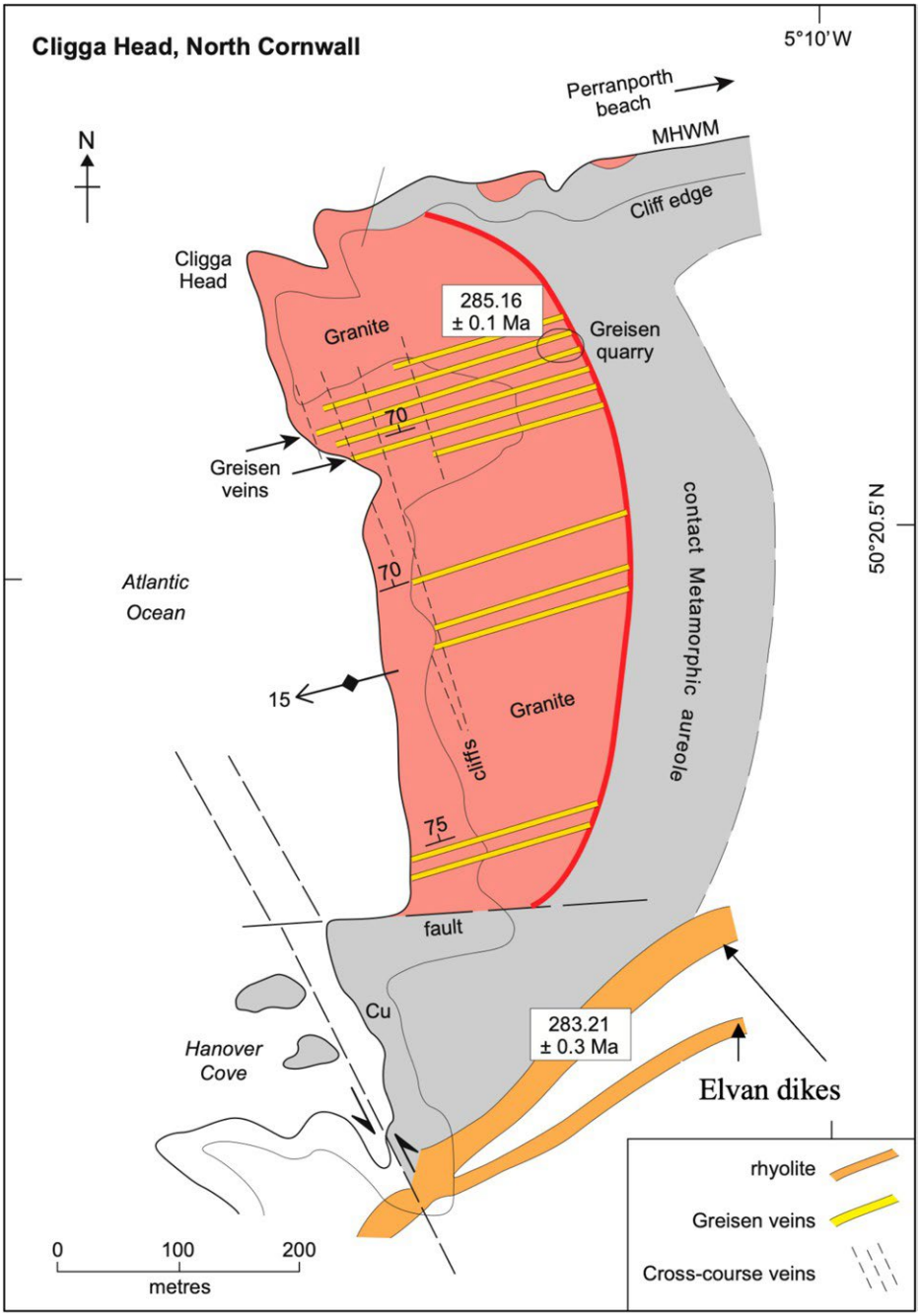

Figure 10. Geological map of Cligga Head region, north Cornwall of SW England, after Moore and Jackson (1977). U-Pb cassiterite age of the granite (285.16 ± 0.1 Ma) and rhyolite dike (283.21 ± 0.3 Ma) are from Tapster and Bright (2020). MHWM—Mean high water mark.

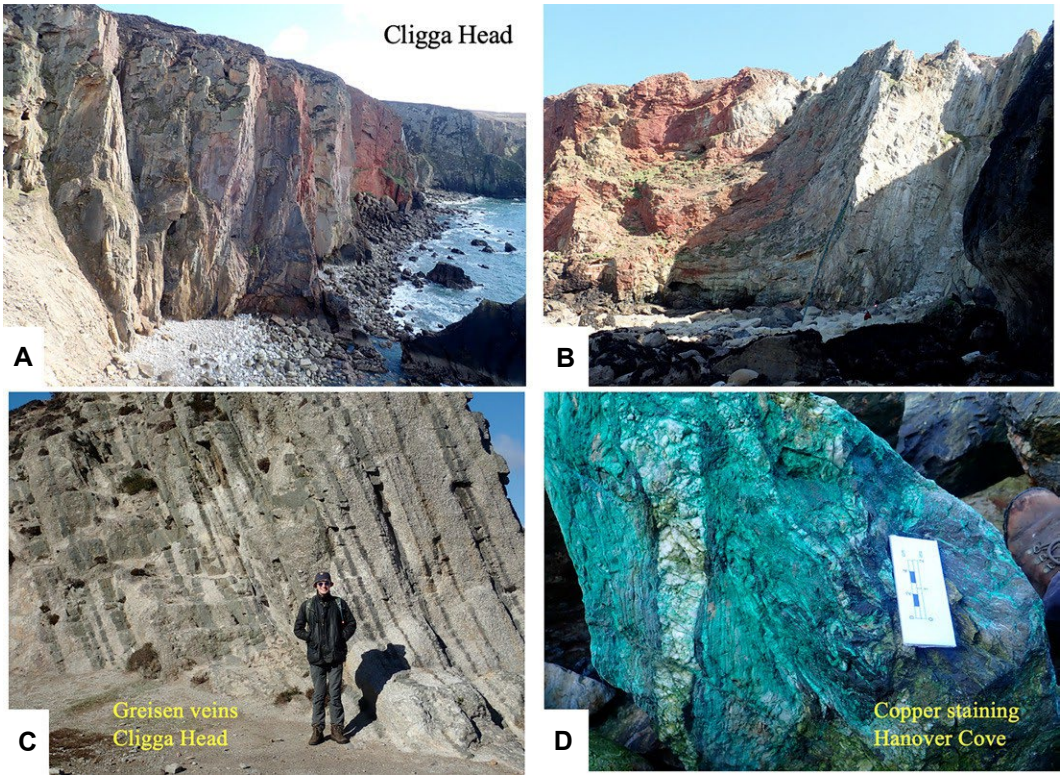

Figure 11. Field relationships, Cligga Head granite of SW England. (A) 90-m-high sea cliffs of Cligga Head granite at low tide. Hanover Cove is at the far end of the beach. (B) Northern margin of the Cligga Head granite showing tin-bearing greisen veins. (C) Tin-bearing tourmaline + muscovite + cassiterite greisen veins intruding the Cligga Head granite. (D) Copper-stained boulders, Hanover Cove.

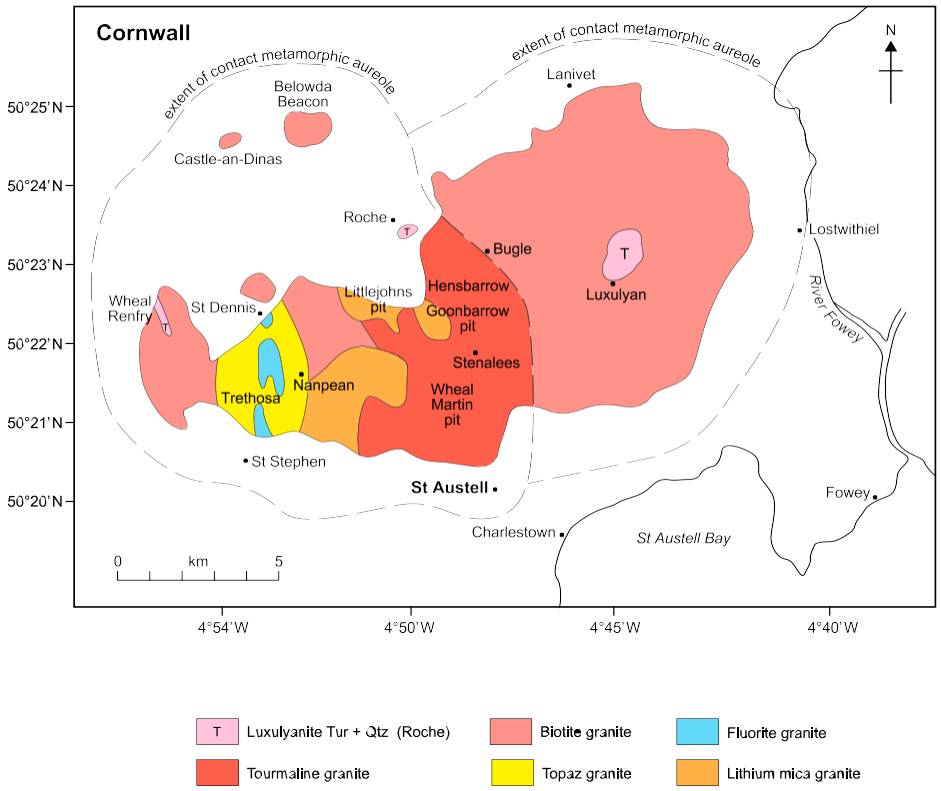

Figure 12. Geological map of the St Austell granite of SW England, after Floyd et al. (1993) and Manning et al. (1996), showing main granite lithologies and key localities mentioned in the text. Qtz—quartz; Tur—tourmaline.

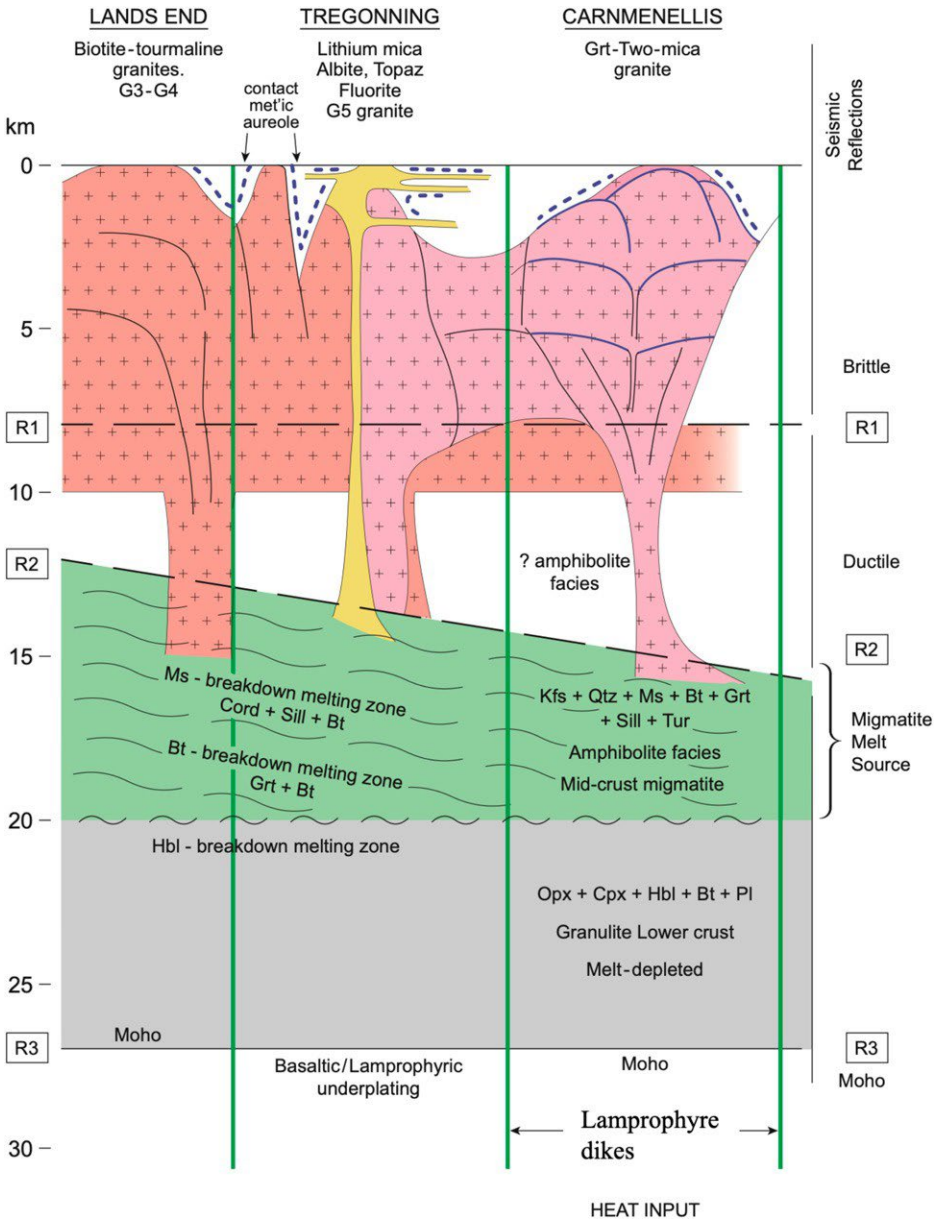

Figure 13. Model for the Land's End, Tregonning, and Carnmenellis granites, SW England. Black dots above the granites are the andalusiteand cordierite-bearing spotted hornfels of the contact metamorphic (met'ic) aureole. R1, R2, and R3 (Moho) are prominent seismic reflectors. The blank area between ~8 km and 12 km depth is inferred to be high-grade amphibolite facies metamorphic rocks and the melting "mush" zone, dominantly comprising sillimanite-grade migmatites. See text for explanation. Bt—biotite; Cord—cordierite; Cpx—clinopyroxene; Grt—garnet; Hbl—hornblende; Kfs—K-feldspar; Ms—muscovite; Opx—orthopyroxene; Qtz—quartz; Sill—sillimanite; Tur—tourmaline.